

The Influence of Pleistocene Megadroughts on Lowland Vegetation in East Africa

Brett T. W. Light

Utrecht University, Faculty of Geoscience
Department of Earth Science: Earth, Life and Climate



First supervisor: Allix Baxter MSc, University of Utrecht, Faculty of Geosciences, PhD Candidate Organic Geochemistry

Second Supervisor: Dr. ir. Francien Peterse, University of Utrecht, Faculty of Geosciences, Assistant Professor of Organic Geochemistry



Table of Contents

Abstract	3
1. Introduction.....	3
1.1 Background and aim of study.....	3
1.2 Using alkanes as paleovegetation indicators	6
1.2.1 Alkane proxies and indices	8
1.2.2 <i>n</i> -alkane $\delta^{13}\text{C}$ values	9
1.2.3 Additional biomarkers	10
1.3 Lake Chala.....	12
1.3.1 Climate.....	13
1.3.2 Vegetation	15
1.3.3 Drill core and age model.....	19
2. Methods	22
2.1 Sample selection	22
2.2 Lipid biomarker analysis	23
2.3 Quantification of compounds	25
2.4 Additionally measured compounds.....	25
2.5 Proxy calculations.....	25
3. Results.....	27
3.1 <i>n</i>-alkane distributions.....	27
3.2. Stable carbon isotopic composition of the <i>n</i>-alkanes	28
3.3 Alkane ratio climate proxies	30
3.4 Alkane proxy trends during the megadrought period 115-98 ka BP	32
4. Discussion.....	33
4.1 Origin of the sedimentary <i>n</i>-alkanes	33
4.2. The terrestrial higher plant $\delta^{13}\text{C}$ signal	35
4.3. Climate control on temporal changes in C_3/C_4 plant contributions	40
5. Conclusion	46
References.....	47

Abstract

Resolving past continental climate variability is important for understanding Earth's climate system, testing climate models and projections of anthropogenic climate change. Here I present a tropical lowland vegetation reconstruction for Eastern Equatorial Africa, for the period 170 to 60 ka covering the African megadrought interval. Based on the stable carbon isotopic composition of terrestrial *n*-alkane leaf-wax biomarkers preserved in Lake Chala, the proportion of C₃ trees and shrubs relative to that of C₄ grasses, remained stable at ~55% and ~45%, despite periods of prolonged and severe aridity that is recorded in the seismic stratigraphic record of the lake sediment. High atmospheric CO₂ concentrations during the Late Pleistocene, enabled C₃ trees and shrubs to outcompete C₄ grasses despite substantial moisture balance variation. This study shows that tropical African vegetation is heavily influenced by climatic moisture balance change on short timescales, though on longer timescales appears to follow the main long-term trend in atmospheric CO₂.

Keywords: *Lake Chala, African Megadroughts, Vegetation, Leaf wax, Alkane, Marine Isotope Stage 5, CO₂.*

1. Introduction

1.1 Background and aim of study

Our knowledge of Earth's dynamic climatic history has come a long way through the use of climate records such as ice sheets and deep-sea cores. These types of climatological archives form an indispensable part of our understanding of the climate history of the past. However, a lack of research from continental and in particular equatorial regions, causes gaps in our understanding as the climate in these areas can be considerably different than that at the poles or oceans. Therefore, it is essential that we develop correspondingly continuous paleoclimate reconstructions within a continental and equatorial context.

Lake sediments often have a high preservation of organic material and are subsequently becoming an important complement to other high resolution

paleoenvironmental archives. Numerous lakes in East Africa have been studied at a variety of timescales such as Lake Tana (Costa et al., 2014), Lake Tanganyika (Felton et al., 2007; Scholz et al., 2007), Lake Victoria (Stager et al., 2017), Lake Malawi (Scholz et al., 2005; Castañeda et al., 2009), Lake Turkana (Morrissey and Scholz 2014) and Lake Albert (Talbot and Brendeland 2001) and have furthered our understanding of the global climate system during the Quaternary period. Investigating African paleoclimates can also provide insights into the evolution and migration of early modern humans (EMH) principally because environmental factors, such as the amount of rainfall, are thought to be one of the governing components behind their dispersions. Additionally, enhancing our understanding of Quaternary climate variability is crucial to resolving long-standing questions about the relative importance of tropical and high-latitude external climate forcing versus local insolation forcing. More than that, it will also reveal to what extent the climatological influences such as temperature, moisture balance and CO₂ shaped past vegetation changes.

The expansion and subsequent dispersion of early modern humans often referred to as the 'Out of Africa' (OOA) theory, is thought to have occurred around 100 ka ago (Grove et al., 2015) and could have been influenced by changes in the climate. Over the past 25,000 years East African climate has responded to changes in Earth's orbit (mainly precession) that influence long term variations in monsoon rainfall and the migration of the intertropical convergence zone (ITCZ) (Tierney et al., 2011; Meyer et al., 2020). The climates of earlier time periods however are less well understood because limited continuous high-resolution terrestrial records exist. Hence, there is a considerable gap in our understanding of equatorial climate change. Numerous studies now show that Eastern Africa underwent several periods of prolonged and severe aridity between 135 and 75 ka ago, termed 'Megadroughts' (Scholz et al., 2007). These presumably had huge implications for the ecology and biodiversity of the region (Cohen et al., 2007; Lyons et al., 2015). The African megadroughts lasted many thousands of years and occurred during the last interglacial (130,000 to 80,000 years ago) across parts of tropical Africa. From the sites investigated thus far, it is commonly understood that they are believed to be of greater severity than any droughts of succeeding time periods (Johnson et al., 2009). These long and intensely dry episodes in the history of African climate are an unexpected phenomenon because their precise timing, origin, and extent have yet to be fully established. It is currently understood that the climate of tropical Africa is dominated by variability in effective moisture, rather than temperature as in higher latitudes, and is

driven by the circulation of the African monsoon and the seasonal migration of the Intertropical Convergence Zone (Scholz et al., 2007). Moisture in East Africa is predominantly obtained from the Indian Ocean (Goddard and Graham, 1999), and the modern precipitation of East Africa has been linked to Indian and Pacific Ocean sea surface temperatures (SSTs) and the El Niño Southern Oscillation (ENSO) (Cane et al., 1994). On the other hand, the long-term forcing of equatorial East African climate has been attributed both to orbital processes (e.g., precession) (Trauth et al., 2003) and to variations in ice volume at high latitudes (Gasse, 2000). This forcing at times is moderated by tropical sea-surface temperatures (SSTs), which may be linked to high-latitude climate processes (Gasse et al., 1989; Street-Perrott and Perrott, 1990). The megadroughts occurred, during a time of eccentricity maxima which also causes a high amplitude of precessional forcing. This forcing brings about heightened seasonality, which typically increases the strength of the monsoon, so the exact timing of these events remains perplexing. These megadroughts are only known because of a few lakes that have records that extend back that far in time and were persistent through large swathes of tropical Africa, including at Lake Chala (Moernaut et al., 2010) and we currently do not fully understand how large of an impact they really had on the landscape. To the South at Lake Malawi (Scholz et al., 2007), in central Africa at Lake Tanganyika (Burnett et al., 2011) and in the far west in Lake Bosumtwi (Scholz et al., 2007) lake levels dropped drastically, often by hundreds of meters. Moreover, these lakes have been shown to be influenced by high latitude climate forcing or other regional specific governing weather phenomenon. For example, an Atlantic influence has been shown to extend well into the western half of the African continent to the Ethiopian highlands, and western portions of the East African Plateau (Tierney et al., 2011); therefore, only in the far east of equatorial Africa can we expect to find a climate history relatively unaffected by a strong northern high-latitude signature. Up to this day, forcing mechanisms of tropical climate in continental areas remain poorly understood. For this reason, and in order to thoroughly understand the implications of these widespread events, we must use a climatological location that is independent of such forcing's.

A newly recovered 214 m composite sediment core from Lake Chala in Eastern Equatorial Africa provides the basis for this thesis. The core dates back to almost 250 ka (Martin-Jones et al., 2019) and therefore, it covers the last two glacial-interglacial cycles and the entire period of human evolution. In this study, will use plant derived lipid biomarkers preserved in the sediments of Lake Chala to investigate the response of vegetation in the East

Africa region to the African megadrought (115-98 ka BP) , to sensitively record the response of vegetation in the East Africa region to these arid intervals. The studied interval covers the time period 60 – 170 ka and thus includes Marine Isotope Stage 5 (MIS5), or the last interglacial period.

In this first chapter, I will introduce the long chain alkanes, which I used to investigate the paleovegetation of Eastern Africa, as well as some proxies based on these lipids. Then I will describe Lake Chala and what is known about the current drivers of its climate. Lastly, I will present the drill core and age model utilized in this study.

1.2 Using alkanes as paleovegetation indicators

Biological markers or biomarkers are molecular fossils, meaning that these compounds originated from formerly living organisms (Shaw and Johns, 1985). Biomarkers are useful because their specific structures reveal more information about their origins than other compounds.

Alkanes which are leaf wax lipids, are a common class of biomarker used to reconstruct changes in both climate and vegetation. Odd-numbered long-chain alkanes $>C_{27}$ are associated with the waxy protective coatings on leaf cuticles and provide protection from infection, physical damage, and desiccation (Eglinton and Hamilton, 1967). Almost all higher plants produce leaf waxes (Eglinton and Hamilton, 1967), and their water insolubility, negligible volatility (for compound with more than 20 carbon atoms), chemical inertness and resistance to biodegradation make them excellent biomarker compounds (Eglinton and Eglinton, 2008).

Alkane biomarkers consist of the elements carbon (C) and hydrogen (H). These molecular compounds are composed of a backbone of carbon atoms also called a carbon skeleton, with hydrogen atoms attached. The carbon atoms are linked by covalent bonds, which are formed when electrons are shared by adjacent atoms. They occur in virtually all-natural settings and show little or no change in structure from their parent organic molecules in living organisms (Eglinton and Hamilton 1967). Almost all higher plants produce leaf waxes (Eglinton and Hamilton, 1967), and their water insolubility, negligible volatility (for compound with more than 20 carbon atoms), chemical inertness and resistance to biodegradation make them excellent biomarker compounds (Eglinton and Eglinton, 2008).

Alkane biomarkers have a straight chain of carbon atoms and consist of the elements carbon (C) and hydrogen (H). These molecular compounds are composed of a backbone of carbon atoms also called a carbon skeleton, with hydrogen atoms attached. The carbon atoms are linked by covalent bonds, which are formed when electrons are shared by adjacent atoms. They occur in virtually all-natural settings and show little or no change in structure from their parent organic molecules in living organisms (Eglinton and Hamilton 1967). Long chain alkanes pass into the environment in and on leaf fragments and aerosols formed from vegetation fires and by wind abrasion. They are often transported long distances by run-off, rivers and air and ultimately deposited and subsequently preserved in lake and marine sediments where they can serve as proxy measures of the continental vegetation that biosynthesized them. An example of plant wax lipids in marine sediments can be seen in figure 1.1 below.

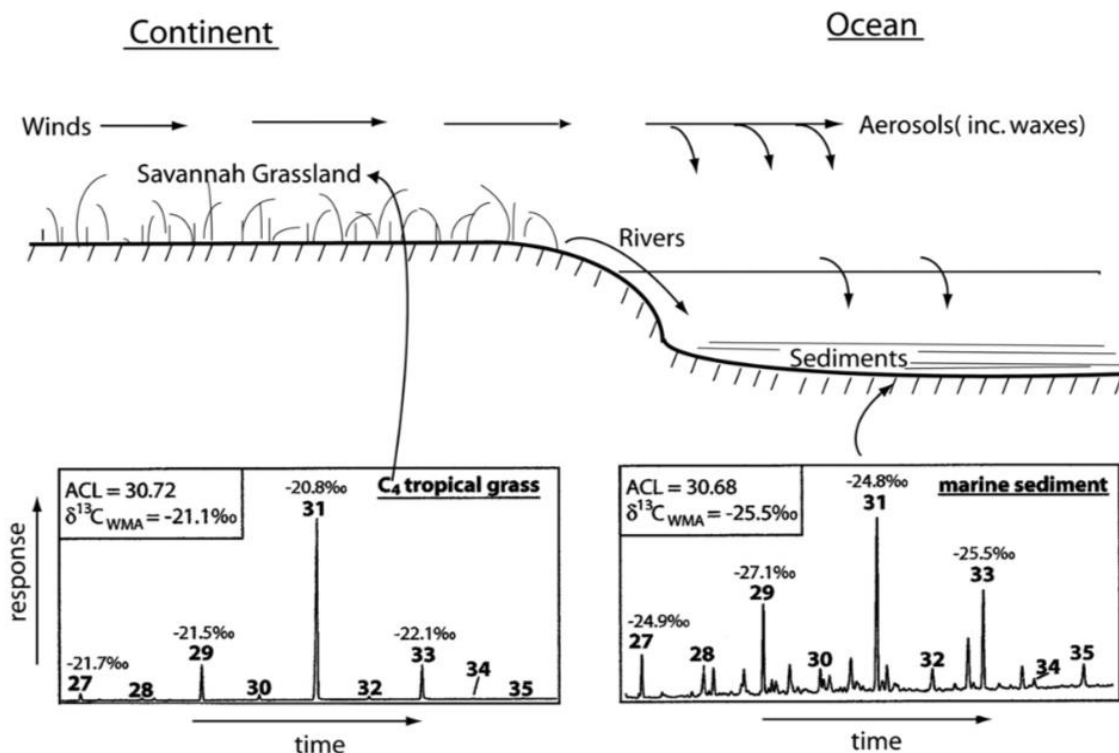


Figure 1.1 An example of plant-wax lipids in marine sediments (Eglinton and Eglinton, 2008). Plant-wax lipids serve as proxies for continental vegetation, since they reach the sediments from the continent, by wind, river transport of particulates and dust and smoke from aerosols. Typical GC traces are shown for the n-alkane fractions (C₂₇-C₃₅) of a C₄ tropical grass and a marine sediment from the Southeast Atlantic (Rommerskirchen et al., 2006). The $\delta^{13}\text{C}$ values (in ‰) are marked for each of the prominent odd-carbon-number homologues and the $\delta^{13}\text{C}_{\text{WMA}}$ (weighted mean average) is also shown for this carbon-number range, together with the Average Chain Length [ACL]. The distribution and isotopic compositions in the marine sediment are in accordance with a significant input of n-alkanes from the African savannah C₄ grassland.

The dominant sources of natural hydrocarbons delivered to aquatic environments include autochthonous sources such as algae and bacteria as well as allochthonous inputs from terrigenous plants (Cranwell, 1982; Meyers and Ishiwatari, 1993; Meyers, 1997). Hydrocarbons from bacterial sources occur in the form of open (noncyclic) chains, generally with carbon chain lengths between C₁₀ and C₃₀. Many studies have attributed even-numbered homologues (C₁₂ to C₂₄) to bacterial sources (Nishimura and Baker, 1986; Grimalt and Albaiges, 1987). Submerged macrophytes often have biomarker compositions intermediate between algae and terrestrial vascular plants. Aquatic macrophytes are generally characterised by a dominance of mid-chain-length *n*-alkanes with odd-numbered homologues. Past studies have shown that submerged and floating aquatic plants have *n*-alkane distributions that maximize at C₂₁, C₂₃ or C₂₅ (Cranwell, 1984; Viso et al., 1993 Ficken et al., 2000). Contrary to bacteria and algae, terrestrial vascular plants are dominated by long-chain *n*-alkanes in the range of C₂₃ to C₃₅. In vascular plants the distribution of *n*-alkanes is usually dominated by odd numbered homologues with C₂₇, C₂₉ and C₃₁ as the dominant compounds. The carbon number at which the *n*-alkane distribution maximises (C_{max}) can sometimes be a diagnostic tracer for different plant sources. Rogge et al, (2007), has used C_{max} as a tool for evaluating the sources of soils deposited to aquatic systems, as some crops differ in their C_{max}.

Different types of terrestrial vegetation produce different distributions of the longer C₂₇-C₃₃ *n*-alkanes; trees and shrubs (C₃ vegetation) typically produce proportionally more of the shorter C₂₇ and C₂₉ *n*-alkanes and grasses (C₄ vegetation) predominantly more of the C₃₁ and C₃₃ *n*-alkanes. Therefore, average chain length can be assumed to be related to water availability, principally because grasses can tolerate higher temperatures and more arid conditions compared to that of trees and shrubs. Aquatic plants typically produce *n*-alkanes with chain lengths of between C₂₁-C₂₅ (Ficken et al., 2000).

1.2.1 Alkane proxies and indices

Long chain (C₂₁ to C₃₇) *n*-alkanes are among the most long-lived and widely utilized terrestrial plant biomarkers (Bush and McInerney, 2013). There have been hundreds of studies examining the range and variation of *n*-alkane chain-length abundances in modern plants from all around the world and *n*-alkane distributions have been used for a variety of purposes

in paleoclimatology and paleoecology as well as chemotaxonomy. This study utilises a few of the most common parameters that are used to describe the n-alkane distributions, namely:

- Average chain length (ACL), The average chain length is the weighted average of the various carbon chain lengths.
- Carbon preference index (CPI). The carbon preference index captures the degree to which odd carbon number n-alkanes dominate over even carbon numbers (Marzi et al., 1993). CPI values greater than 1 mean a predominance of odd over even chain lengths since biologically odd n-alkanes are preferred. In the course of diagenesis and catagenesis, however, even n-alkanes are produced by conversion processes, so that the value approaches 1 with increasing maturity.
- Aquatic macrophytes proxy (Paq) Aquatic macrophytes are generally characterised by a dominance of mid-chain-length n-alkanes, intermediate between algae and terrestrial vascular plants. Paq, expresses the relative contributions of these plants versus emergent and terrestrial plant input into lake sediments (Ficken et al., 2000).
- Chain length ratio (C29/C31). The chain length ratio of C29/C31 is postulated to reflect the sedimentary contributions of woody plants to that of grasses.

The proxy calculations are discussed in more detail in chapter 2.5.

1.2.2 *n*-alkane $\delta^{13}\text{C}$ values

The $\delta^{13}\text{C}$ values of carbon atoms in the wax molecules depends on that of the ambient atmospheric CO_2 , the pathway employed during photosynthesis, and on factors (including aridity) that affect the conductance of the plant's stomata (Street-Perrott, 1997). Higher plants use two fundamentally different pathways for CO_2 fixation: the C_3 (Calvin-Benson) and the C_4 (Hatch-Slack) cycles. The Hatch-Slack cycle pre-concentrates CO_2 before it is fixed by the enzyme Rubisco, culminating in an ecological advantage in arid, hot or low $p\text{CO}_2$ conditions (Aucour et al., 1994 and Street-Perrott, 1997). The pre-concentration of CO_2 generates significantly less isotopic discrimination which results in less depleted $\delta^{13}\text{C}$ values of the biomass (O'Leary et al., 1992) and wax lipids (Collister et al., 1994) of C_4 plants compared to C_3 plants. Bulk C_4 plant $\delta^{13}\text{C}$ values range from -9 to -15‰ (averaging -12.5‰), while C_3 plant values range from -22 to -37‰ (averaging -27‰) (O'Leary, 1988). C_3 plants

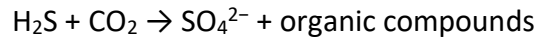
comprise most temperate species, including grasses, trees and shrubs. C₄ species are much less numerous and are typically tropical grasses and sedges. The overall average distributions and isotopic composition of the *n*-alkanes differ clearly between those two plant types, even though there is considerable interspecific variation within each (Eglinton and Eglinton, 2008). One can use measures such as leaf wax alkane patterns and compound-specific carbon isotope analysis of fossil lipids in complex mixtures of organic matter, for the reconstruction of the predominant pathway of CO₂ fixation used by plant species constituting to the regional vegetation (Huang et al., 2001 and Schefuß et al., 2003). In turn these findings can be taken as a reflection of the growth environment and, hence, the climate controlling it. In spite of this, there are complexities in interpreting δ¹³C at the compound-specific level, since individual plants displayed a range of values (Collister et al., 1994). Mechanisms for the diverse array of isotopic signatures in primary producers likely arise from reaction kinetics and carbon metabolism (Bianchi and Canuel, 2011).

1.2.3 Additional biomarkers

Many aquatic systems contain diverse organic matter sources, and the application of different chemical biomarkers has provided a useful tool for tracing their source and environmental fate. Plant pigments are one class of biomarkers that have widely been used as tracers for phytoplankton sources in aquatic systems (Duan and Bianchi, 2006) and have been used in aquatic paleoecology to better understand historical changes in bacterial community composition, trophic levels, redox change, acidification of lakes and past levels of ultraviolet (UV) radiation (Leavitt and Hodgson, 2001). The primary photosynthetic pigments used in absorbing photosynthetically active radiation (PAR) are chlorophylls, carotenoids and phycobillin's; with chlorophyll representing the dominant photosynthetic pigment (Clayton, 1980). Carotenoids are tetraterpenoids, made by bacteria algae, fungi and higher plants generally consisting of a C₄₀ chain with conjugated double bonds (Goodwin, 1980). There are also some carotenoids made by certain bacteria that are composed of C₃₀, C₄₅ and C₅₀ chains, but these represent a small percentage of the estimated 600 carotenoid structures identified (Bianchi and Canuel, 2011). One carotenoid discussed in this study Isorenieratene.

Isorenieratene is a carotenoid light harvesting pigment with the chemical formula C₄₀H₄₈ (Damsté et al., 2001). It is produced by green sulphur bacteria (*Chlorobium*) which

perform photosynthesis using hydrogen sulphide rather than water, shown in the equation below:



Anoxygenic photosynthesis requires reduced sulphur (and therefore strictly anaerobic conditions) and light. Green sulphur bacteria are commonly found in meromictic lakes and ponds, sediments, and some sinkholes. These constrained basin environments usually have a very stratified water column and steep density gradients. The presence of Isorenieratene and its derivatives in sediments are useful when studying the carbon cycle, as this type of biomarker indicates photic zone anoxia (Brocks et al., 2005).

Isoarborinol, a pentacyclic triterpenoid alcohol, as well as arborinone, its ketonic counterpart have been observed, often in substantial amounts, in some ancient immature and contemporary sediments, particularly of lacustrine origin (Albrecht and Ourisson, 1969). Transformation products of isoarborinol/arborinone have also been reported in tropical lakes (Jaffe and Hausmann, 1994). Transformation products of isoarborinol/arborinone including: the mono-, di- and tri-unsaturated des-A-arborene have been reported in the 25,000-year sedimentary record of Lake Chala (van Bree et al., 2018). These compounds are known in a few angiosperm species, including *Gramineae* (Ohmoto and Ikuse, 1970) and in one case from a lichen (Gonzalez et al., 1991) and initially were thought to be possible markers of higher plant organic matter (Albrecht and Ourisson, 1969). However, due to both their abundance in some sediments and their peculiar structural features, they were later suggested to be of microbial origin (Ourisson et al., 1982; Volkman, 2005). The transformation of isoarborinol and arborinone to the different des-A-arborenes depends on enzymatic action. Its likely that the microbial community that produces these products, is influenced by subtle spatial variation in the water-column environment and thereby the structures and relative abundances of des-A-arborenes in the sediment (van Bree et al., 2018). Microbial communities will be most different in different lake systems, they may also be contrasting within one system, where they will differ seasonally and along a depth gradient. Although these microbial changes are likely to occur on short spatial and temporal timescales, sediments can record these cumulatively in the form of long-term trends, and hence examining absolute and relative changes in sedimentary des-A-arborenes degradation products through time provide insight into some physical aspects of a lake system.

A study by van Bree et al. (2018) looked at possible palaeoclimatological and environmental controls on the concentrations of des-A-arborenes and compared them against two independent proxy records of climatic moisture balance (the precipitation/evaporation ratio), the seismic-reflection record of lake level fluctuation and the branched isoprenoid tetraether (BIT) index of past rainfall variations. The concentration of des-A-arborenes was found to be somewhat higher during inferred wetter periods and lower during inferred drier periods. While no specific evidence for a mechanistic link explaining this relation was provided by this study it is inferred that des-A-arborenes production must have been higher during times of more pronounced water-column stratification and/or higher precipitation.

The branched isoprenoid tetraether (BIT) index has more recently been shown to actually correspond to the position of the oxycline which is related to stratification within a lake system (Baxter et al., 2021), and this is associated to the strength of the monsoonal winds. Lower wind speeds associated with rainy periods result in weaker mixing and higher BIT values conversely, higher monsoonal wind speeds are associated with dry conditions generate more extensive mixing of the upper water column and this generates lower BIT values. Principally because the position of the oxycline within a lake determines the anoxic habitat of GDGT-0 and brGDGT producers relative to that of the crenarchaeol producers.

1.3 Lake Chala

Lake Chala (3.3° S, 37.7° E) is a relatively small ca. (4.5km²) and deep (94m) crater lake situated in a steep-sided volcanic basin on the border between Kenya and Tanzania, East Africa (figure 1.3). The lake formed approximately 250,000 years ago (Dieleman et al., 2018), after a monogenetic parasitic eruption associated with Mt Kilimanjaro's most recent phase of volcanic activity (Martin-Jones et al., 2019). The region in South-Eastern Kenya is part of the East African plateau, which at mean surface elevations between 500m and 1500m is dotted with mountain ranges associated with the Eastern Rift Valley and the Eastern Arc (Sinninghe Damsté et al., 2011). The lake is located at an altitude of 880m on the S.E. slope of Mt. Kilimanjaro, 8 kilometres north of Taveta, Kenya, and 55 kilometres east of Moshi, Tanzania. The geology of the area is typical of extrusive volcanic rock terrane. The extrusive volcanic

rocks terminate against basement igneous and metamorphic rocks about 3.2 km to the east of Lake Chala (Payne 1970).

The lake is surrounded by a steep crater rim with a maximum height of 170m (Wolf et al., 2014) and has an additional catchment area of ca. 1.43 kilometres (Buckles et al., 2018). Surface inflow to the lake is limited to run-off from the steep inner crater slopes, except for a narrow 300m long ravine which breaches the crater's north-western rim and is active during infrequent heavy thunderstorms. The lake's water budget is also influenced by sub-surface in and outflow too. Subsurface inflow originates from rainfall on the upper flanks of Mt. Kilimanjaro, that enters the lake from a shallow groundwater aquifer. Sub-surface outflow is estimated to amount to ~2.5% of lake volume annually (Payne, 1970). More significant outflow through porous upper crater walls probably starts ~10 m above the 2003 lake level, the upper limit of shallow caves eroded by wave action during past high stands.

The lakes surface temperature varies seasonally but on average is around 22.2°C. Daily wind-driven mixing of the water column is limited to 15-20 m and deep mixing of the water column extends down to 40-60 m between June and September, when air and surface temperatures are lowest (Van Bree et al., 2014). The bottom water of the lake is permanently anoxic that the lower water column is permanently stratified, or at most mixes at a decadal or lower frequency (Wolff et al., 2011). Allochthonous organic matter in Lake Chala sediments consists of wind-blown particles from the surrounding savanna landscape, augmented by soil erosion and litter input from the inner crater rim (Damste et al., 2011).

1.3.1 Climate

The local climate is tropical semi-arid with air temperatures lowest during northern hemisphere summer (June – August) and highest during northern hemisphere winter (November - March). Monthly mean daytime temperatures ranging from 26 °C in July – August to 30°C in February – March. Rainfall in the region is highly seasonal due to the twice-annual passage of the Inter Tropical Convergence Zone (ITCZ). The twice-yearly passage of peak insolation, and thus the zone of maximum convective activity over the region, creates a bimodal pattern of seasonal rainfall (Moernaut et al., 2010). The wet seasons are warmer and less windy than the main dry season of June to September (Barker et al., 2009), with a south-easterly monsoon bringing 'long rains' from March to mid-May and the north-easterly monsoon bringing 'short rains' from late October to December (Figure 1.2c). At the town of

Taveta 10km south of Lake Chala, mean annual rainfall is 583mm/yr^{-1} , with the long and short rains contributing on average to 48% and 31% of the annual total respectively (1982-2005; data courtesy of the Taveta weather station). The precipitation/evaporation (P/E) balance of lake Chala is highly negative, estimated to be around 600mm/yr rainfall and around 1700mm/yr lake-surface evaporation (Payne, 1970).

Seasonal and long-term variation in East African rainfall reflects shifts in the latitudinal position of the tropical rain belt linked to the Intertropical Convergence Zone (ITCZ), (Mamalakis et al., 2021). The ITCZ is the region that circles the Earth, near the equator, where the trade winds of the Northern and Southern Hemispheres come together (figure 1.2.a). It migrates meridionally in response to changes in interhemispheric heat distribution. Additionally, the intensity and movement of the ITCZ itself is driven largely by variation in Indian Ocean Sea Surface Temperatures (SSTs), which in turn determines the strength of monsoonal dynamics delivering rainfall to eastern Africa (Leng et al., 2019).

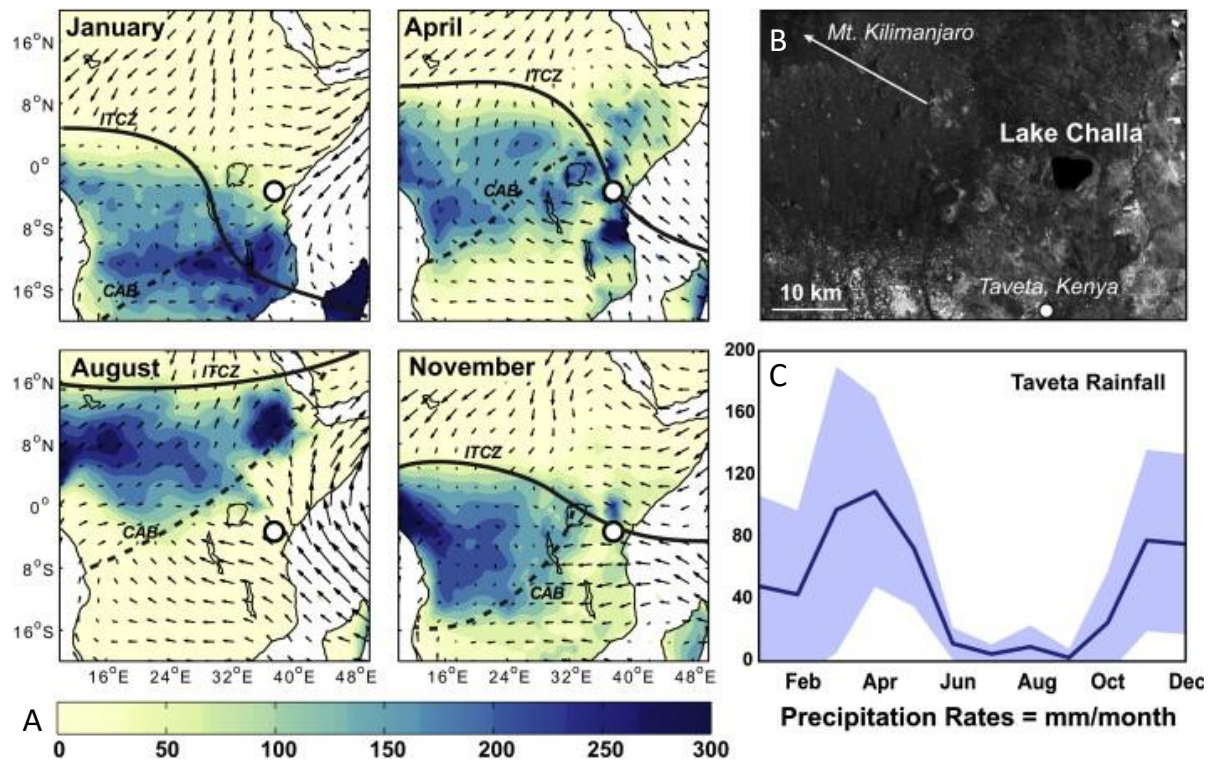


Figure 1.2 (A) Climatology of tropical Africa for four representative months including precipitation rates (mm/month), and the approximate locations of the Inter-tropical Convergence Zone (ITCZ) and Congo Air Boundary (CAB). The white dot represents the location of lake Chala. (B) An aerial photo of Lake Challa which is located on the eastern flank of Mt. Kilimanjaro at 880 m above sea level. (C) Average monthly precipitation rates (average mm/month over the period 1978-2005, with standard deviation) from the nearby town of Taveta, Kenya. (Tierney et al., 2011). Note the Congo Air Boundary (CAB), a convergence zone that marks the confluence of Indian Ocean air with unstable air from the Congo Basin, lies well to the west of Lake Chala at all times of the year (Tierney et al., 2011).

1.3.2 Vegetation

The Lake Chala region in South-Eastern Kenya is part of the East African plateau. Apart from moist coastal woodland near the Indian Ocean (Figure. 1.3a), natural vegetation at elevations up to ~ 1500 m mostly consists of deciduous wooded grassland and bushland with 15–40% crown cover (White, 1983), adapted to a tropical monsoonal climate with pronounced seasonal drought. In the surrounding area of the lake a large percentage of the land has been converted to agriculture. Most of the closed woodland and substantial amounts of the open wooded grassland has been converted to rainfed tree (banana), shrub (coffee) and herbaceous (maize and wheat crops), intermixed with vegetable gardens (hatched areas fig. 1.3c). However, the open bush and grass savanna with scattered trees and shrubs in the immediate vicinity of the lake is relatively undisturbed (fig. 1.3c). The relatively dense tree

cover on the northern and western outer slopes of the crater, is defined as a dry colline savanna forest with *Acalypha fruticosa*, *Grewia* and *Acacia* (Hemp, 2006), and along the nearby Lumi and Tsavo rivers and in (seasonally dry) stream gullies occur strips of moist evergreen riverine forest (White, 1983). Inside the crater below the main cliff faces is a rocky shoreline which is occupied by a narrow strip of evergreen forest. A dry but dense 'succulent' forest with *Commiphora baluensis*, *Haplocoelum foliolosum* and *Euphorbia bussei* occurs on steep middle slopes between the cliffs and the crater rim, and gentle higher slopes below the crater rim are covered in open grassland with scattered trees and shrubs (Sinninghe Damsté et al., 2011).

A 2007 botanical survey of the Chala basin, identified 31 families and 107 species of trees, shrubs and herbs, excluding grasses and sedges (S. M. Rucina, National Museums of Kenya, unpublished data 2007). Fourteen species are from families in which some species (1–5% of the total) are C₄ plants: Acanthaceae, Asteraceae, Boraginaceae and Euphorbiaceae. However, the only local non-grass genus in which C₄ photosynthesis is known to occur is *Heliotropium* of the Boraginaceae, and it has been documented in only six of its 250 known species (Sage et al., 1999). Full vegetational data for the Chala region is incomplete, on the other hand it is expected to show very similar patterns of C₄ prevalence as Kruger National Park in South Africa. This is because it experiences a similar annual rainfall, a 4 month long dry season and it also has a vegetation of open woodland, bush and grassland with *Acacia*, *Combretum* and *Grewia* among the most common trees (Sinninghe Damsté et al., 2011). A study by Codron et al., 2005 of the vegetation in Kruger National Park found all local trees and 94% of the local herbs to be C₃, and all grasses were C₄. Among sedges, the ratio was 75% C₃ vs. 25% C₄. Having said that, sedges are virtually absent around Lake Chala due to lack of suitable riparian habitat along its steep rocky shores (Sinninghe Damsté et al., 2011).

One potentially complicating factor in the context of this study, is the relatively high local abundance of succulent plants in the genera *Euphorbia*, *Sansevieria* and *Aloe*. The tree-like *E. bussei*, in particular, is a signature species of dry forest occupying the steep middle slopes inside Chala crater. These succulent C₃ plants employ CAM (Crassulacean Acid Metabolism) photosynthesis; where CO₂ uptake and temporary fixation occurs at night, allowing the stomata to remain closed during the day as an adaptation to high temperatures and seasonal aridity. CAM plants can have $\delta^{13}\text{C}$ values similar to those of C₄ plants (Sage et al., 1999) and in Kruger National Park, they were indistinguishable (Codron et al., 2005). CAM

plants like these could bias the linear mixing model that is used later on in this study and perhaps overestimate the proportion of C₄ vegetation at times.

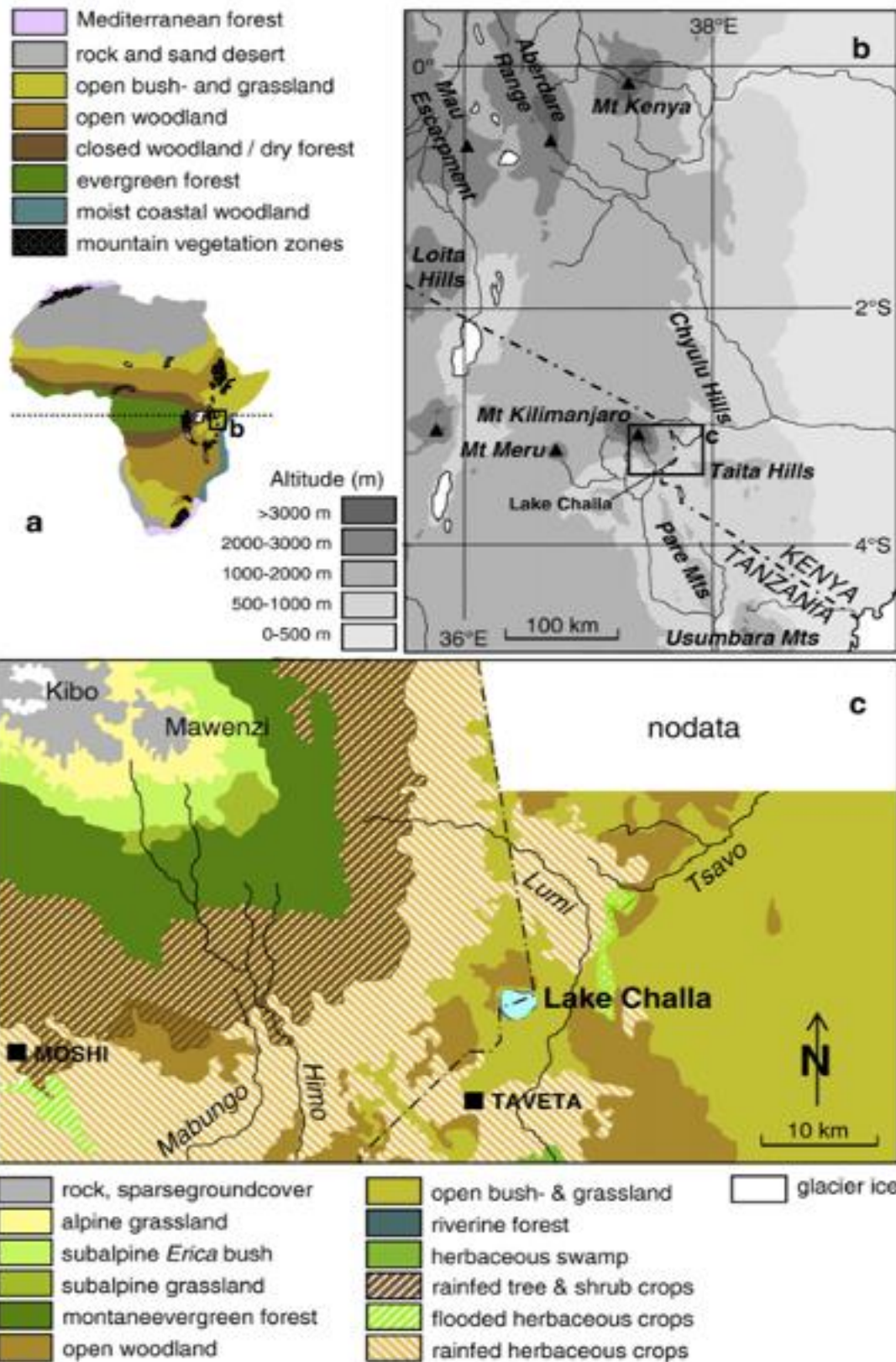


Figure 1.3 Maps of Lake Chala in equatorial East Africa, (A) regional vegetation cover, (B) regional topography and (C) local vegetation cover (Sinninghe Damsté et al., 2011). Note the hatched areas indicate that >50% of the land use is under agriculture.

1.3.3 Drill core and age model

In November 2016, as part of the International Continental Scientific Drilling Program, the DeepCHALLA project (Verschuren et al., 2013) retrieved a 215 m long sediment record from Lake Chala. The sedimentary sequence, comprised of mostly finely laminated organic muds, had a recovery rate of 100% in the upper 121.3 m (160,000 years), and an 85% recovery rate of the lower section. The lowest part of the core, a layer consisting of volcanic sand and silt was deposited around 260,000 years ago (Verschuren et al., 2013). The separate cores are linked by tie points based on sedimentary features (mainly turbidites) to create the final composite core that covers the last 260,000 years, including the two most recent glacial-interglacial cycles.

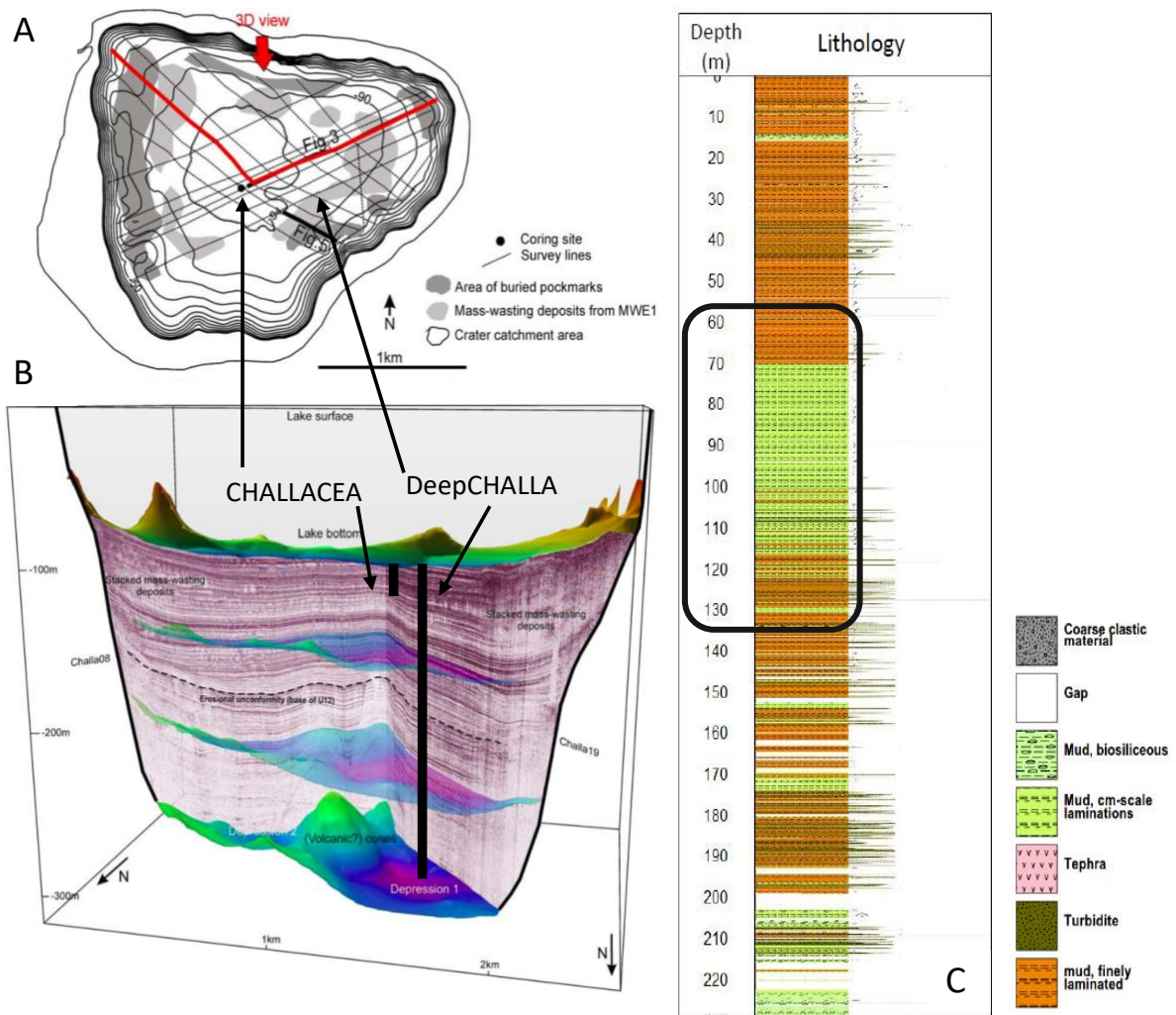


Figure 1.4 Location of the CHALLACEA and DeepCHALLA drill cores. (A) Lake Chala and its crater catchment area, with bathymetry and location of the core sites in relation to seismic survey lines (Moernaut et al., 2010). (B) 3D representation of Lake Chala's sedimentary infill, as viewed from the north. (C) Lithology of the 2016 DeepCHALLA core, (Verschuren, 2019 unpublished) (black box) denotes the section of core analysed in this study.

The DeepCHALLA core consists of finely laminated varved muds on the (mm) scale as well as thicker laminated muds on the (cm) scale, biosiliceous mud, coarse clastic material, turbidite and tephra (figure 1.4c). Sonic velocity data shows that there is little compaction throughout the core and that the lower section of the core is still watery (Verschuren, 2019 unpublished). This study utilises the interval 133 – 59 m of the DeepCHALLA core in which the lithology, consisted of mostly finely laminated varved muds on the cm and mm scale, alternate. Marked transitions in the core occur at around 123 m, where larger mm scale laminations are replaced

by cm scale laminations and again at 70 m where the cm laminations are replaced again by more finely laminated sediments (figure 1.4c).



Figure 1.5 Image of sections of the Lake Chala core from ICDP website (<https://www.icdp-online.org/projects/world/africa/lake-challa-kenya-tanzania/>).

The preliminary age model for the DeepCHALLA sequence (figure 1.6) is primarily based on radiocarbon dating, seismic data and the position of the Toba ash at ~75 ka BP. The age model utilises links between Lake Chala seismic stratigraphy and known near global climate events back to 140 ka (Moernaut et al., 2010); and an extrapolation of the average sedimentation rate over this 140-ka interval (0.80 m/ka) to the base of the DeepCHALLA sequence (Martin-Jones et al., 2019).

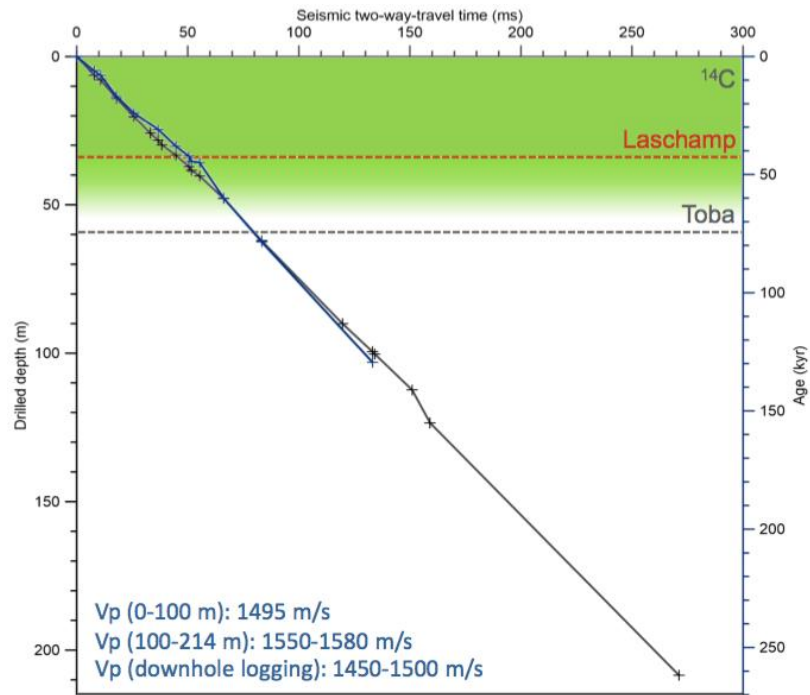


Figure 1.6 Preliminary age model for the DeepCHALLA composite core, based on the tie points between sedimentary features (turbidites and tephra) and the age model for the 140-ka period based on seismic stratigraphy (Moernaut et al. 2010). The near constant sonic velocity (V_p) implied by that cross-correlation and measured in down-hole logging, both indicating very little compaction with increasing depth (Verschuren et al., 2017). (Source: research poster available online at: <http://pastglobalchanges.org/download/docs/pdf/verschuren-poster-pages17.pdf>).

2. Methods

2.1 Sample selection

Seventy samples were selected from the DeepCHALLA sediment core covering the depth interval 49.68m - 133.53m, corresponding with the time period 170.7 - 60.58 thousand years (BP) (Figure, 2.1). This interval encompasses the observed drought 98-115 ka BP, as seen in the seismic-stratigraphic record of lake-level fluctuations (Moernaut et al., 2010) (Fig. 2.1A), and overlaps with periods of prolonged aridity in other regions of Africa at this time, as discussed in the previous section.

A targeted sampling approach was employed, in order to record the alkane distributions across the megadrought (fig. 2.1B), while also covering the periods of climate transition beforehand and afterwards. Samples outside of the megadrought period were selected at a higher resolution in order to identify the vegetation composition at the transitions leading into and out of the drought, while a lower resolution was used to track changes during the most arid phase.

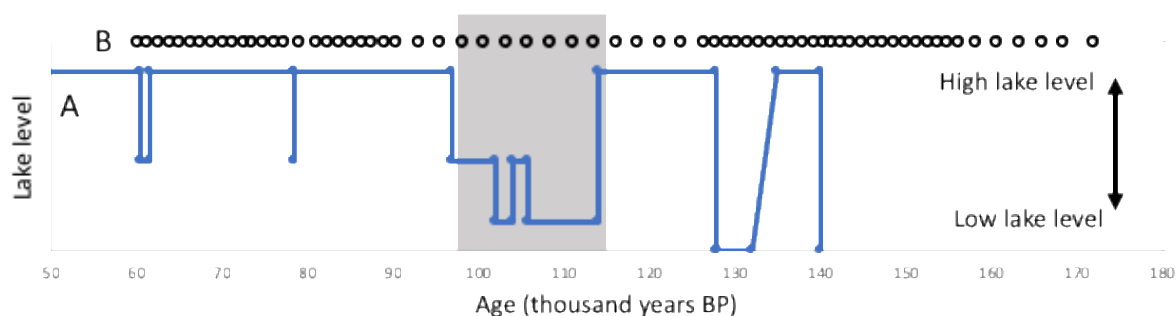


Figure 2.1 (A) Lake level reconstruction of Lake Chala (blue line) based on seismic reflection data (Moernaut et al., 2010). (B) A visual representation of the targeted sampling method, (black circles) denote the analysed sediment intervals. The grey shaded area is the drought, as recognised in the seismic-stratigraphic record of lake-level fluctuations (Moernaut et al., 2010).

The time period 60-89 kyr consists of 23 samples with an average age resolution of 1315 years, the period 90-125 kyr consists of 14 samples with an average age resolution of 2574 years, the period 126 – 155 kyr consists of 24 samples with an average age resolution of 1242 years and the period 156 - 172kyr consists of 7 samples with an average age resolution of 2611 years.

2.2 Lipid biomarker analysis

Lipid extraction

Between 7 g and 2 g of wet core sediment was freeze dried and powdered. The freeze-dried and powdered sediments were extracted with a Dionex™ Accelerated Solvent Extractor (ASE) using a dichloromethane (DCM)/methanol (9:1, v/v) mixture at high temperature (100°C) and pressure (7.6×10^6 Pa). The total organic extracts were separated over a column with

activated Al₂O₃ into an apolar and polar fraction using hexane/DCM (9:1, v/v) and DCM/MeOH (1:1, v/v) as eluents respectively.

Removal of elemental sulphur with Copper

Elemental sulphur present in the apolar fractions was removed prior to analysis of *n*-alkanes. Copper turnings were activated by adding a small amount of 2N Hydrochloric acid (HCL). The acid was then removed, and distilled water was added until the pH of the water was neutral. The copper turnings were then washed twice with a small amount of methanol (MeOH) followed by dichloromethane (DCM). A small amount of activated copper turnings was added to the apolar fraction along with 3 ml of DCM and stirred overnight. Subsequently, the DCM layer was passed over a small Na₂SO₄ column to remove the formed CuS.

Separation of saturated and unsaturated hydrocarbons

Silver coated silica was used to separate the saturated and unsaturated hydrocarbons in the apolar fractions using hexane and ethyl acetate as eluents, respectively.

Alkane analysis

The saturated apolar fraction of the total lipid extract (TLE) was analysed for *n*-alkanes, specifically long chained alkanes of lengths 23-35 carbon atoms long. The *n*-alkanes were analysed on a Hewlett-Packard (HP6890 series) gas chromatograph (GC) equipped with an on-column injector and flame ioniser detector (FID). The samples were dissolved in hexane and 1ul was injected. The samples were injected at 70°C with an oven temperature programme of increasing temperature by 20°C min⁻¹ until reaching 130°C and then at 4°C min⁻¹ until reaching 320°C, at which it was held for 20 minutes. The GC was equipped with a fused silica capillary column (25 m x 0.32 mm) coated with CP Sil CB (film thickness 0.12 µm) and helium was used as carrier gas. The performance of the GC was monitored daily using an internal standard of a known concentration. The samples were co-injected with 1 ul of squalene (C₃₀H₅₀) of a known concentration.

Biomarker identification

A selection of samples was also analysed on a GC-Finnigan Trace DSQ mass spectrometer (GC-MS) for compound identification. The samples were dissolved in hexane and 1ul was injected.

The instrument was equipped with a fused silica capillary column as described above for the GC. The carrier gas was helium, and the same oven temperature program as for GC was used. The MS operated at 70 eV with a mass range of m/z to 40 to 800 and a cycle time of 1.7 s. The performance of the machine was monitored daily using an internal standard of a known concentration.

Compound specific isotope analysis

The *n*-alkanes were subject to compound-specific $\delta^{13}\text{C}$ analysis using an Agilent 6800 GC coupled to a ThermoFisher Delta V isotope-ratio monitoring mass spectrometer (GC-IRMS). The $\delta^{13}\text{C}$ values were measured against calibrated external reference gas and performance of the instrument was measured by daily injections of a mixture of C_{20} and a C_{24} perdeuterated *n*-alkane with known isotopic compositions. The $\delta^{13}\text{C}$ values are reported in the standard delta notation against the Vienna Pee Dee Belemnite (VPDB) standard.

2.3 Quantification of compounds

Quantification of the *n*-alkanes, des-A-arborenes and Isorenieratene was performed by peak area integration of the GC chromatograms and dividing this by the peak area integration value of the co-injected squalene standard of a known concentration. The concentration of these compounds was calculated using the peak area of the internal standard and normalized to the amount (g) of organic carbon (C_{org}) in each sample.

2.4 Additionally measured compounds

The concentrations of Des-A-arborenes were measured during this study as they have been previously reported in the sediments of Lake Chala to be associated with moisture balance. The presence of Isorenieratene was also measured although not quantified. Isorenieratene is a proxy for photic zone anoxia that is usually associated with constrained basin environments. It could provide additional information on the lake conditions around the time of the megadrought.

2.5 Proxy calculations

The following equations were used to calculate:

Average chain length (ACL)

$$\text{ACL} = [(C_{23} \times 23) + (C_{24} \times 24) + (C_{25} \times 25) + (C_{26} \times 26) + (C_{27} \times 27) + (C_{28} \times 28) + (C_{29} \times 29) + (C_{30} \times 30) + (C_{31} \times 31) + (C_{32} \times 32) + (C_{33} \times 33) + (C_{34} \times 34) + (C_{35} \times 35)] / (C_{23} + C_{24} + C_{25} + C_{26} + C_{27} + C_{28} + C_{29} + C_{30} + C_{31} + C_{32} + C_{33} + C_{34} + C_{35}).$$

Carbon preference index (CPI)

$$\text{CPI} = 0.5 \times [(C_{25} + C_{27} + C_{29} + C_{31} + C_{33}) / (C_{26} + C_{28} + C_{30} + C_{32} + C_{34}) + (C_{25} + C_{27} + C_{29} + C_{31} + C_{33}) / (C_{24} + C_{26} + C_{28} + C_{30} + C_{32})].$$

Aquatic macrophytes proxy (P_{aq})

$$P_{\text{aq}} = (C_{23} + C_{25}) / (C_{23} + C_{25} + C_{27} + C_{29}).$$

Weighted average ($\delta^{13}\text{C}_{\text{wax}}$)

$$\delta^{13}\text{C}_{\text{wax}} = [(C_{29} \times \delta^{13}\text{C}_{29}) + (C_{31} \times \delta^{13}\text{C}_{31}) + (C_{33} \times \delta^{13}\text{C}_{33}) + (C_{35} \times \delta^{13}\text{C}_{35})] / (C_{29} + C_{31} + C_{33} + C_{35}).$$

C₂₉/C₃₁

$$C_{31} / (C_{29} + C_{31}).$$

3. Results

3.1 n-alkane distributions

All analysed sediments contained a suite of long chain ($C_{23} - C_{35}$) *n*-alkanes with a strong odd over even carbon preference. An example chromatogram trace is shown in figure 3.1 below.

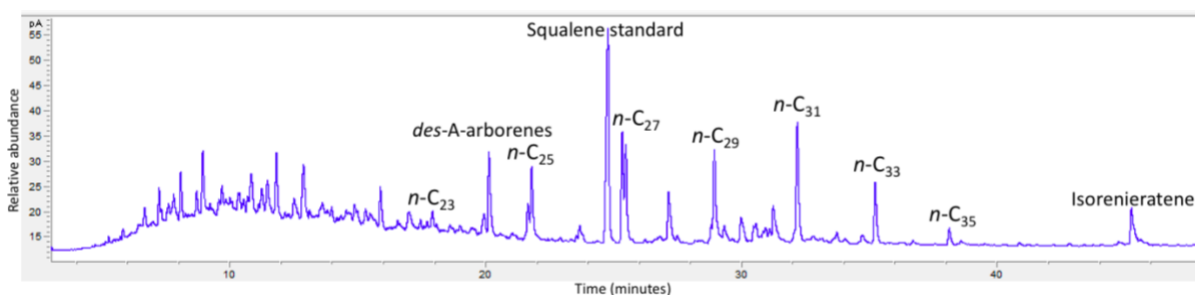


Figure 3.2 A gas chromatogram (GC) trace of sample JR0213 (depth – 101.56 m / age 128.762 kyr BP). The alkane carbon number, des-A-arborenes, Isorenieratene and the internal standard (squalene) are also indicated.

The concentrations of the $C_{23} - C_{35}$ *n*-alkanes extracted from the sediments of Lake Chala show large variance between 170.7 – 60.6 kyr BP (figure 3.2).

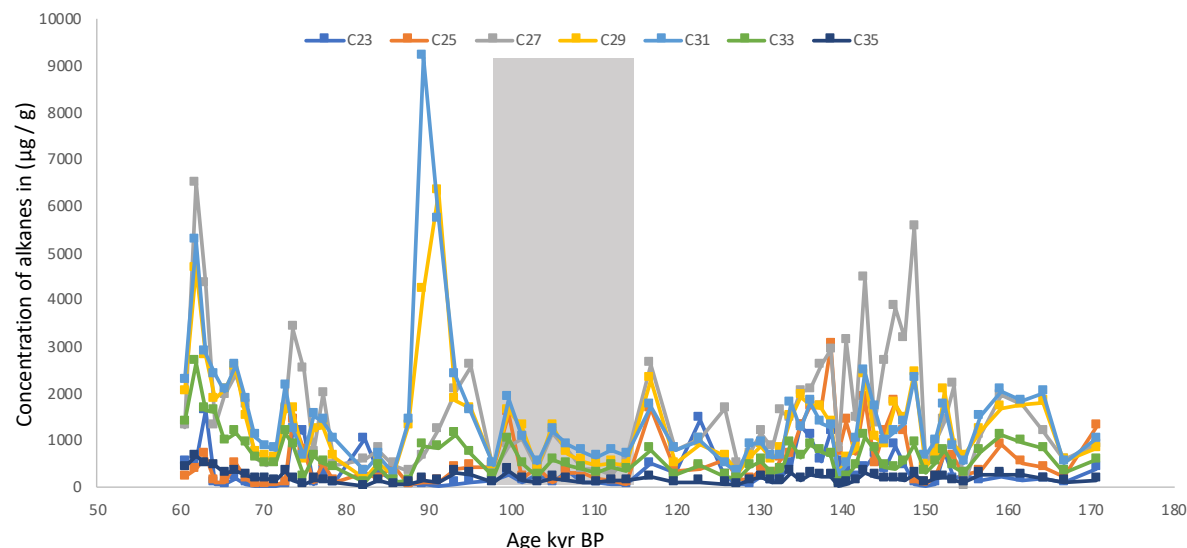


Figure 3.3 Concentration of odd carbon number of alkanes $C_{23} - C_{35}$ in ($\mu\text{g} / \text{g}$) of dry sediment. The grey shaded area is the drought, as recognised in the seismic-stratigraphic record of lake-level fluctuations (Moernaut et al., 2010).

The C_{23} *n*-alkane concentrations varied from 14 – 1633 $\mu\text{g} / \text{g}$, the C_{25} *n*-alkane from 42 – 3028 $\mu\text{g} / \text{g}$, the C_{27} *n*-alkane from 247 – 6481 $\mu\text{g} / \text{g}$, the C_{29} *n*-alkane from 193 – 6304 $\mu\text{g} / \text{g}$

g, the C₃₁ *n*-alkane from 238 – 9184 µg / g, the C₃₃ *n*-alkane from 59 – 2654 µg / g and the C₃₅ *n*-alkane from 25 – 649 µg / g.

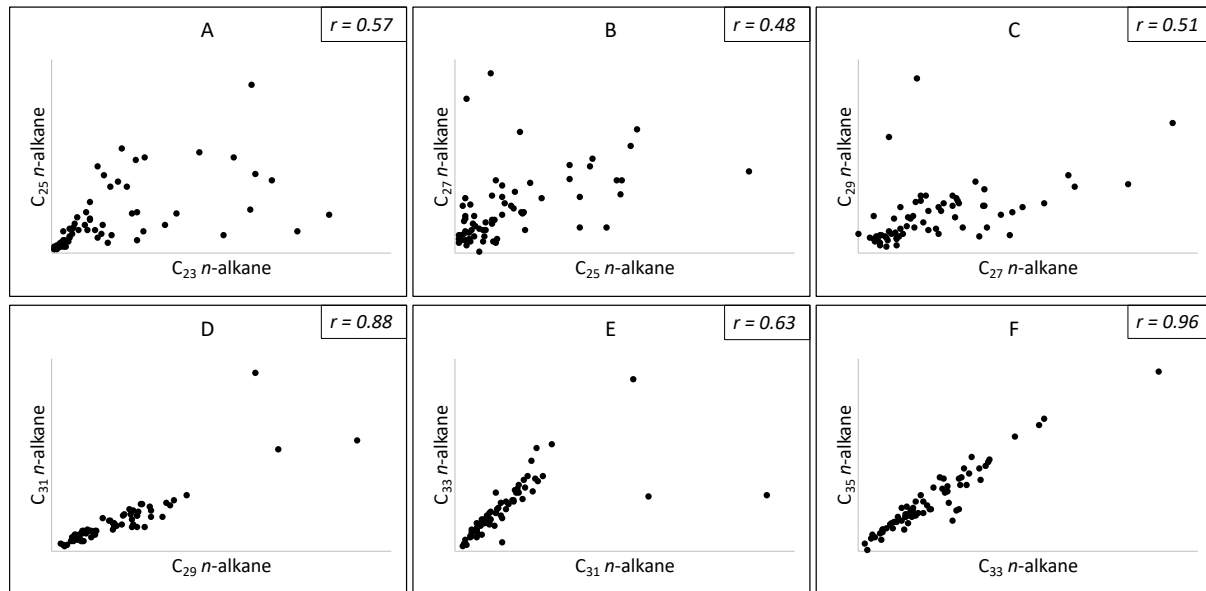


Figure 4.3 Scatter plots of *n*-alkane concentrations plotted against one another, showing the visual correlation between sequential *n*-alkane lengths: (A) *n*-alkane C₂₃ and C₂₅, (B) *n*-alkane C₂₅ and C₂₇, (C) *n*-alkane C₂₇ and C₂₉, (D) *n*-alkane C₂₉ and C₃₁, (E) *n*-alkane C₃₁ and C₃₃ *n*-alkane and (F) *n*-alkane C₃₃ and C₃₅. The correlation coefficient (*r* - value) displaying the strength and direction of the relationship is also indicated.

The concentrations of shorter length *n*-alkanes (*n*-C₂₃, *n*-C₂₅ and *n*-C₂₇) show the least amount of correlation to the next; indicated by low correlation coefficient (R-values); 0.57, 0.48 and 0.51 respectively (figure 3.3a, b, c). The longer chain length *n*-alkane concentrations (*n*-C₂₉, *n*-C₃₁, *n*-C₃₃, and *n*-C₃₅) show a much stronger relationship to the next (fig. 3.3d, e, f), with R values of 0.88, 0.63, and 0.96. This indicates that the shorter chain length *n*-alkanes (*n*-C₂₃, *n*-C₂₅ and *n*-C₂₇) likely originate from mixed sources. The similar proportionate concentrations of the longer *n*-alkanes (*n*-C₂₉, *n*-C₃₁, *n*-C₃₃, and *n*-C₃₅), indicate they are likely from similar sources.

3.2. Stable carbon isotopic composition of the *n*-alkanes

The stable carbon isotopic composition ($\delta^{13}\text{C}$) of the C₂₃ - C₃₅ *n*-alkanes extracted from the sediments of Lake Chala shows large variance between 170.7 – 60.6 kyr BP (figure 3.4).

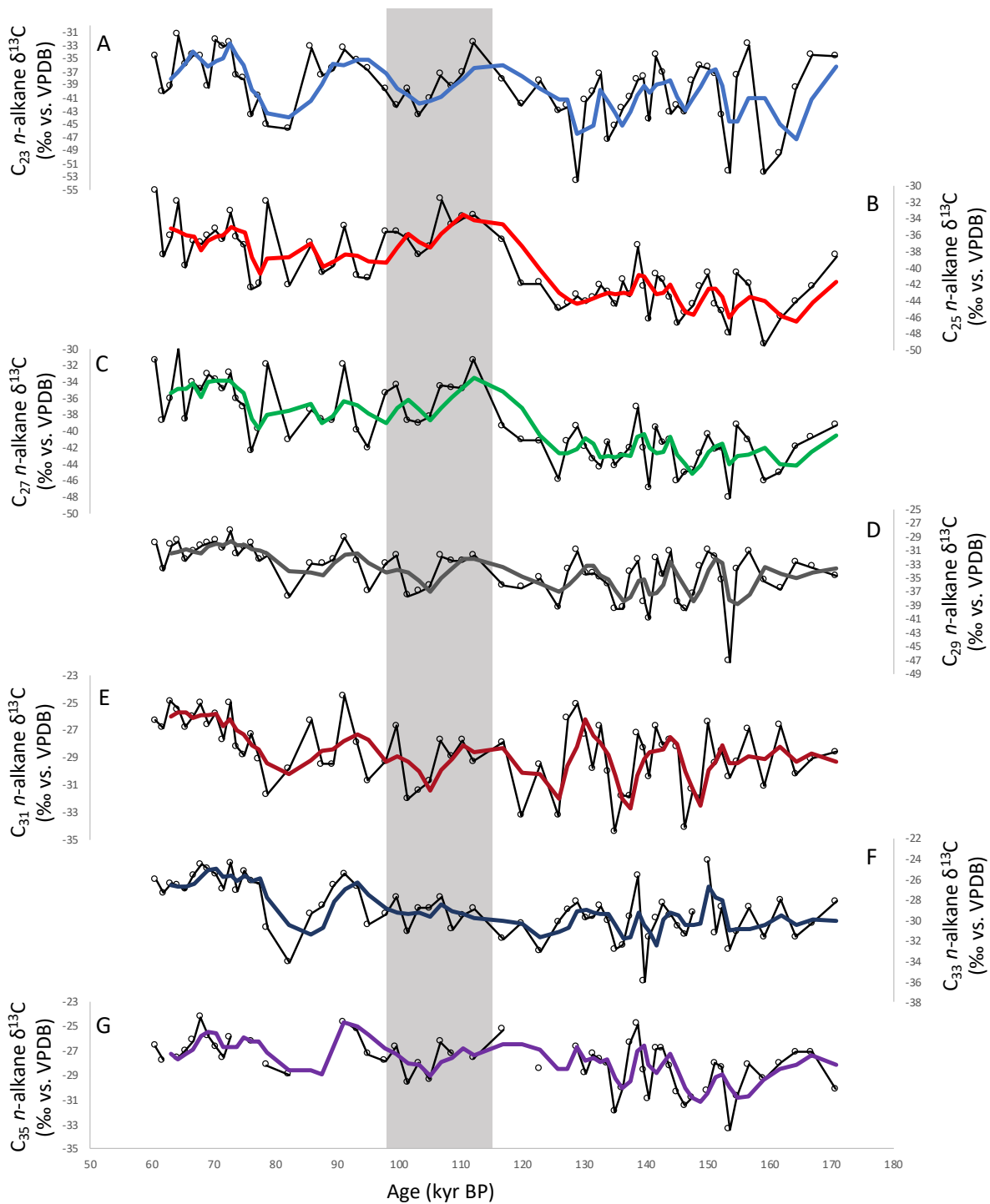


Figure 3.5 Stable carbon isotopic compositions (in ‰ vs. VPDB) of seven different analysed *n*-alkanes extracted from the sediments of Lake Chala over the period 170.7 - 60.6 kyr BP. (A) The C₂₃ *n*-alkane. (B) The C₂₅ *n*-alkane. (C) The C₂₇ *n*-alkane. (D) The C₂₉ *n*-alkane. (E) The C₃₁ *n*-alkane. (F) The C₃₃ *n*-alkane. (G) The C₃₅ *n*-alkane. The three-point moving average (thick coloured lines) in A-G are superimposed on the *n*-alkane records (thin black lines). The grey shaded area is the drought, as recognised in the seismic-stratigraphic record of lake-level fluctuations (Moernaut et al., 2010).

The variance of $\delta^{13}\text{C}$ values in the $n\text{-C}_{23}$ alkane ($\delta^{13}\text{C}_{\text{C}23}$) from the deepCHALLA core is from -53.7‰ to -31.5‰,

the $n\text{-C}_{25}$ alkane ($\delta^{13}\text{C}_{\text{C}25}$) is from -49.4‰ to -30.6‰,

the $n\text{-C}_{27}$ alkane ($\delta^{13}\text{C}_{\text{C}27}$) is from -48.1‰ to -29.9‰,

the $n\text{-C}_{29}$ alkane ($\delta^{13}\text{C}_{\text{C}29}$) is from -47.3‰ to -28.1‰,

the $n\text{-C}_{31}$ alkane ($\delta^{13}\text{C}_{\text{C}31}$) is from -34.4‰ to -24.5‰,

the $n\text{-C}_{33}$ alkane ($\delta^{13}\text{C}_{\text{C}33}$) is from -36.0‰ to -24.2‰,

the $n\text{-C}_{35}$ alkane ($\delta^{13}\text{C}_{\text{C}35}$) is from -33.4‰ to -24.3‰ (figure 3.4).

The shorter chain length n -alkanes ($n\text{-C}_{23}$ and $n\text{-C}_{25}$) have the most depleted $\delta^{13}\text{C}$ values, and to a lesser extent the mid length n -alkanes ($n\text{-C}_{27}$ and $n\text{-C}_{29}$) also have depleted values. The longer chain n -alkanes ($n\text{-C}_{31}$, $n\text{-C}_{33}$ and $n\text{-C}_{35}$) have the least depleted $\delta^{13}\text{C}$ values. The $\delta^{13}\text{C}$ of the $n\text{-C}_{23}$ alkane varies the most and the $\delta^{13}\text{C}$ of the $n\text{-C}_{31}$ alkane varies the least (figure 3.4).

3.3 Alkane ratio climate proxies

There is large variance in all the measured proxies from the analysed interval between 170.7 – 60.6 kyr BP (figure 3.5).

The carbon preference index (CPI) varied between 2.1 and 30.0 (fig. 3.5a).

The aquatic macrophytes proxy (P_{aq}) varied between 0.02 and 0.85 (fig. 3.5b).

The average chain length (ACL) varied between 26.1 and 30.3 (fig. 3.5c).

The chain length ratio (C29/C31) varied between 0.39 and 0.69 (fig. 3.5d).

The concentration of the des-A-arbores varied between 91 and 51,327 ng/ g dry weight sediment (fig. 3.5e). The weighted average proxy ($\delta^{13}\text{C}_{\text{wax}}$) varied between -25.6 and -37.6‰ (fig. 3.5f)

Isorenieratene although not quantified, was found in 7 of the analysed sediment intervals (fig. 3.5g).

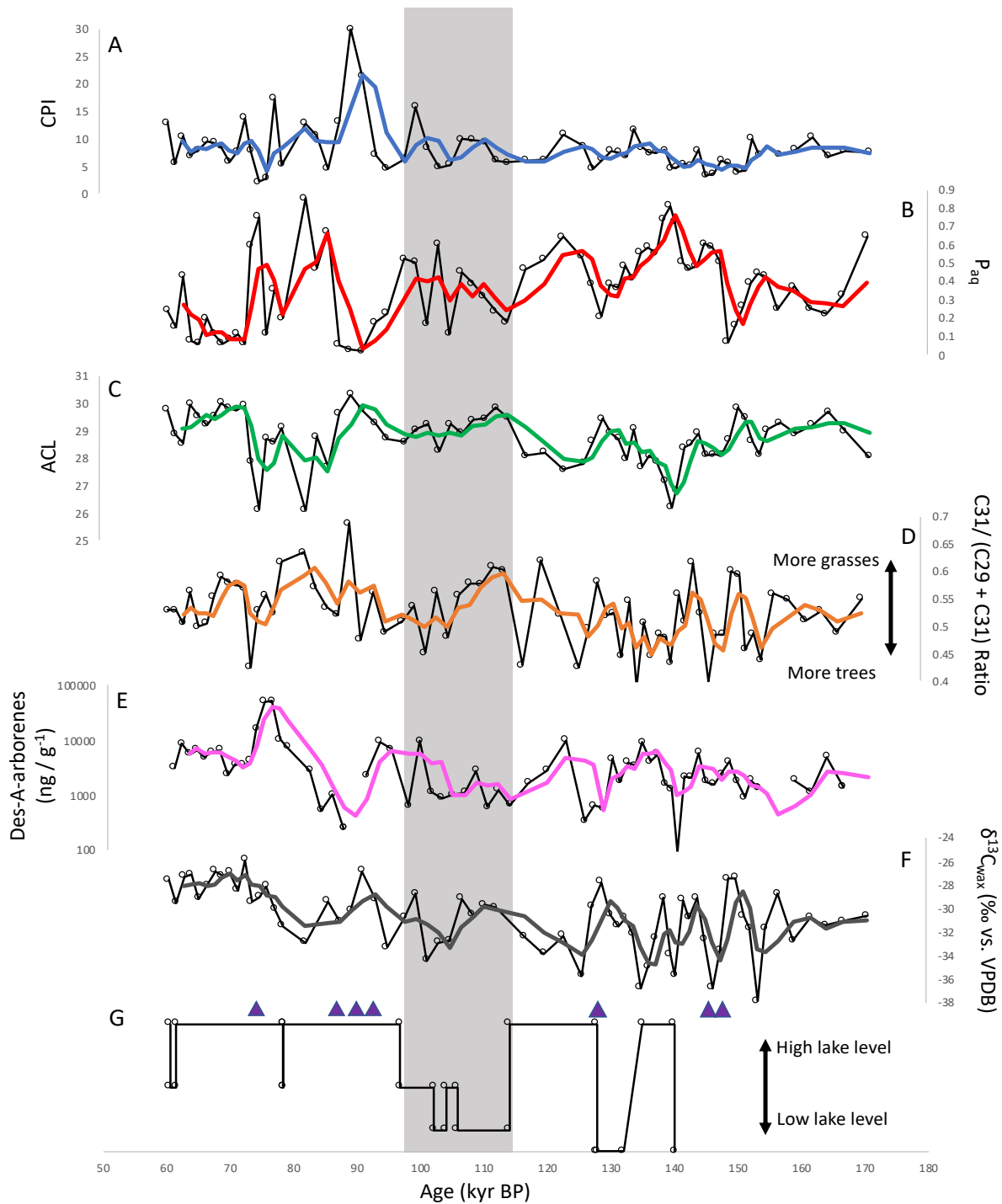


Figure 3.6 Biomarker and *n*-alkane proxy data based on organic biomarkers extracted from the sediments of Lake Chala over the period 170.7-60.6 kyr BP. (A) Carbon preference index (CPI), a measurement of the relative abundance odd over even carbon chain lengths and captures the degree to which odd carbon number *n*-alkanes dominate over even carbon numbers. (B) Aquatic macrophytes proxy (P_{aq}), a proxy ratio formulated to reflect the non-emergent aquatic macrophyte input to lake sediments relative to that from the emergent aquatic and terrestrial plants. (C) Average chain length (ACL) is the weighted average of the

various carbon chain lengths (C_{23} - C_{35}). (D) $C_{31}/(C_{29}+C_{31})$ ratio, is a chain length n -alkane parameter that can be used as a paleovegetation proxy, to distinguish the relative contributions of C_3 (trees) and C_4 (grasses). (E) Concentration of Des-A-arbores (ng / g⁻¹ dry wt) microbial degradation products of angiosperm plant triterpenoids. (F) $\delta^{13}C_{wax}$ (‰ vs. VPDB), a proxy which reflects the $\delta^{13}C$ contributions of the higher plants. (G) The seismic-stratigraphic record of lake-level fluctuations in Lake Chala (Moernaut et al., 2010), plotted with the presence of Isorenieratene (purple triangles), a pigment of the photosynthetic green sulphur bacteria Chlorobiaceae, an indicator for photic zone anoxia (Koopmans et al., 1996). The thin black lines in (A-F) are the proxy records and the (thick coloured lines) represent a three-point moving average. The grey shaded area is the drought, as recognised in the seismic-stratigraphic record of lake-level fluctuations (Moernaut et al., 2010).

3.4 Alkane proxy trends during the megadrought period 115-98 ka BP

The carbon preference index values remain quite stable during the megadrought period (figure 3.5a), they do vary between 15.8 and 4.8, meaning that there was a strong odd over even predominance at all times. Aquatic macrophytes proxy (P_{aq}) that is formulated to reflect the non-emergent aquatic macrophyte input to lake sediments relative to that from the emergent aquatic and terrestrial plants does show variability. It ranges from 0.60 to 0.11, which signifies that at times non-emergent aquatic macrophytes constitute a meaningful contribution to the sedimentary n -alkane record. The average chain length is trending lower from the start of the megadrought period until the end, ACL values measure 29.84 at the beginning and 28.57 towards the end. This implies that there is a greater contribution of C_3 vegetation to the sedimentary n -alkane record across this interval. Also supporting the establishment of greater C_3 vegetation at this time is the chain length ratio (C_{29}/C_{31}), because it is also trending lower across the megadrought interval with values ranging from 0.60 to 0.50. Trending upwards across the megadrought interval is the concentration of the des-A-arbores, as discussed in section 1.2.3 their concentration in the sediments of Lake Chala is related to moisture balance, and this indicates that it is getting wetter throughout the megadrought time period. Lastly the $\delta^{13}C_{wax}$ is for the most part is trending more negative across the megadrought period, suggesting that there is an increase in the proportion of C_3 vegetation.

4. Discussion

4.1 Origin of the sedimentary *n*-alkanes

Long-chain ($>C_{23}$) *n*-alkanes in lake sediments can derive from a number of sources. Terrestrial higher plants in the vicinity of the lake can be a major source as almost all terrestrial plants are covered with a wax layer that in many instances comprises of long-chain *n*-alkanes with a strong odd over even carbon predominance (Eglinton and Hamilton, 1967). Plant waxes can be transported via wind, soil run-off, or river (Scheffé et al., 2003b; Simoneit, 1977). In case of Lake Chala with its vegetated crater rim and absence of river input, the plant waxes are likely to derive predominantly from the local vegetation (Sinninghe Damste et al., 2011). Some plants have a pedicular *n*-alkane pattern, nevertheless, because of the high number of potential contributors, the distributions extracted from lake sediments represent averages of many plant species. The wax lipids of plants from different types of tropical African vegetation have been studied in great detail (Rommerskirchen et al., 2006; Vogts et al., 2009; 2012). The variability between *n*-alkane distributions of the different analysed plant taxa within each type of vegetation is substantial. Though, the *n*-alkane distributions of (mostly C_3) rainforest plants tend to maximize at $n-C_{29}$, whereas *n*-alkane distributions of C_3 savanna trees and shrubs and C_4 grasses, have a maximum at $n-C_{31}$.

A second source of *n*-alkanes in lake sediments, can come from aquatic higher plants living in the lake itself. Non-emergent (submerged and floating-leaved) macrophytes are often characterized by high relative abundance of C_{23} and C_{25} *n*-alkanes (Ficken et al., 2000). Emergent aquatic plants, which in tropical African lakes are often reed (*Phragmites* sp.), or papyrus and other tall sedges (*Cyperus* spp.), display *n*-alkane distributions similar to those of terrestrial vegetation, typically dominated by higher ($>C_{29}$) homologues (Ficken et al., 2000; Mead et al., 2005). One way to examine the contributions of emergent and non-emergent aquatic macrophytes in lake sediments is to use the biomarker ratio P_{aq} . The premise of the biomarker ratio P_{aq} , is that it represents the contribution of non-emergent aquatic macrophytes to fossil *n*-alkanes in the sediments (Ficken et al., 2000). In the sediments of Lake Chala the contributions of the C_{23} and C_{25} *n*-alkanes are at times significant, P_{aq} reaches its maximum value of 0.85 at 82.17 (kyr) ago (figure 3.5b). These are similar contributions to those reported for surface sediments of very shallow lakes in other parts of tropical East Africa. Lake Nkunga and Lake Sacred (Kenya) for example, support a high density of

submerged and floating leaved aquatic plants (Ficken et al., 2000), so these seemingly high P_{aq} values nevertheless may suggest a contribution of such plants to the sedimentary n -alkanes, at least during some periods. On the other hand, no shallow-bottom littoral habitat occurs in the present-day Lake Chala, and even substantial lake level lowering inferred from seismic data (Moernaut et al., 2010) is unlikely to have created more favourable conditions for establishment of aquatic macrophytes. Therefore, it seems unlikely that submerged/floating leaved aquatic plants are the origin of these isotopically depleted n -C₂₃ or n -C₂₅ in Lake Chala sediments.

A different origin for the C₂₃ and C₂₅ n -alkanes is visible from their $\delta^{13}C$ values, which are considerably more negative than those of the C₂₉-C₃₅ n -alkanes (Fig 3.5). Even though the $\delta^{13}C$ values of wax lipids in various species of submerged and floating leaved plants show considerable variation (Ficken et al., 2000; Mead et al., 2005), this fails to constrain the origin of the C₂₃ and C₂₅ n -alkanes in Lake Chala. The $\delta^{13}C$ values for the C₂₃ and C₂₅ n -alkanes of common macrophytes, such as *Hydrilla* sp., *Nymphaea nouchali*, *Potamogeton thunbergi*, and *Utricularia reflexa* in the Mt. Kenya lakes varied from -27.3 to -33.2‰ , with *U. reflexa* displaying the most depleted values (Ficken et al., 2000; Mead et al., 2005). The somewhat lighter carbon isotopic signal for *Utricularia* species could be due to its lifestyle, feeding on insects of which the carbon is likely depleted in ^{13}C . The very light $\delta^{13}C$ values of C₂₃ and C₂₅ n -alkanes in Lake Chala sediments would suggest that they may partially derive from *Utricularia* species. On the other hand, *Utricularia* is generally only found in nitrogen-limited marshy shallow lakes (Denny, 1985) and a 2008 vegetation survey of 36 crater lakes in Uganda with diverse pH and littoral habitat, *Utricularia* was found only in one atypical, low-pH swampy lake (Damsté et al., 2011). In the present-day Lake Chala, *Utricularia* is not found, therefore, it is very unlikely that *Utricularia* species are the source of these isotopically depleted C₂₃ and C₂₅ n -alkanes in Lake Chala sediments. To conclude, the n -alkane distributions in Lake Chala sediments reflect two different sources. Both the C₂₃ and C₂₅ n -alkanes are isotopically distinct from the other n -alkanes, and despite the C₂₃ alkane being reported as dominant in non-emergent aquatic plants this appears to be an unlikely explanation for Lake Chala. The higher (>C₂₉) n -alkanes derive predominantly from terrestrial plants in the vegetation surrounding Lake Chala.

The n -alkane distributions of organisms are often not limited to one or two individual components (Eglinton and Hamilton, 1963) For this reason, it is likely that the ^{13}C -depleted

isotopic signature of the n -C₂₃ and n -C₂₅ of unknown origin is also partly reflected in the carbon isotopic composition of the higher n -alkanes. Certainly, the n -C₂₇ and, to a lesser extent, the n -C₂₉ are characterized by more depleted $\delta^{13}\text{C}$ values than the C₃₁ - C₃₅ n -alkanes (Figure 3.4), suggesting that the C₂₇ and C₂₉ n -alkanes are of mixed origin. In spite of this, both the ACL and P_{aq} did not show any relationship with the $\delta^{13}\text{C}$ of the C₃₁ n -alkane (Figure 4.1), indicating that the source of isotopically depleted n -alkanes did not affect the $\delta^{13}\text{C}$ signature of the n -C₃₁.

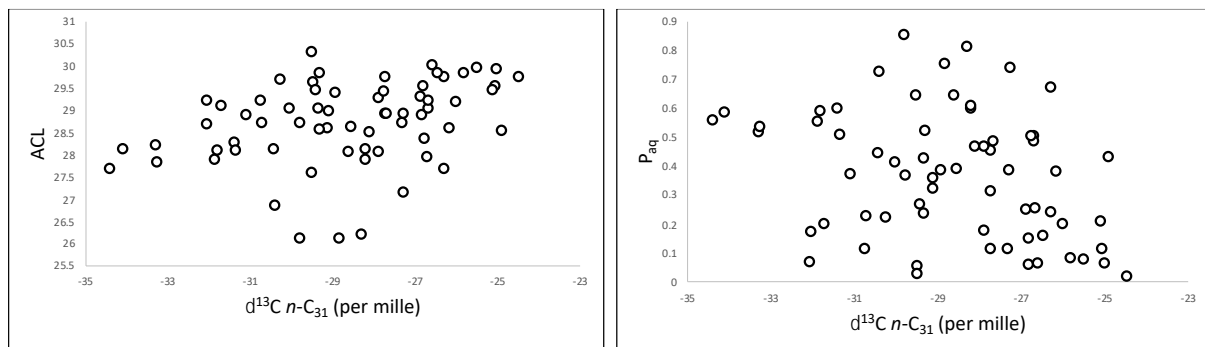


Figure 4.1 Cross plots of the ACL and P_{aq} with the $\delta^{13}\text{C}$ of the C₃₁ n -alkane. The absence of any relationship indicates that the source of isotopically depleted C₂₃ and C₂₅ n -alkanes did not affect the $\delta^{13}\text{C}$ signature of n -C₃₁.

4.2. The terrestrial higher plant $\delta^{13}\text{C}$ signal

In the previous section, I explained that the C₃₁-C₃₅ n -alkanes in Lake Chala sediments primarily originate from terrestrial higher plants. From the suite of alkanes I measured, the C₃₁ n -alkane generally had the highest abundance, meaning that its stable carbon isotopic composition could be measured most precisely. It is also the most abundant n -alkane in C₃ trees/shrubs and in C₄ grasses of present-day African savanna vegetation (Vogts et al., 2009), and its $\delta^{13}\text{C}$ value is not affected by the source of isotopically depleted C₂₃ and C₂₅ n -alkanes (figure 4.1). I therefore used the isotopic composition of this n -alkane as an indicator for changes in the terrestrial plant community surrounding Lake Chala. A two-member mixing model was used to estimate the %C₄ plant contribution to the sedimentary n -C₃₁ based on average $\delta^{13}\text{C}$ values for n -C₃₁ in C₃ plants (-35.2‰) and C₄ plants (-21.7‰) from a compilation of literature data (Castañeda et al., 2009). This reveals a vegetation record that shows large variance over the whole-time interval of this study. The n -C₃₁ alkane ($\delta^{13}\text{C}_{\text{C31}}$) lowest value is

-34.4‰ and its highest value is -24.5‰ (figure 3.4), a $\delta^{13}\text{C}$ variance of 9.9‰. At the beginning of the megadrought interval (116.8 kyr BP), the percentage of C_4 vegetation was around 54%, this decreased to 24% at 101.4 kyr BP. The maximum C_4 vegetation is 63% at 99.6 kyr BP and towards the end of the arid interval \sim 43% at 97.8 kyr BP. This indicates a significant change in the terrestrial higher plant population from a mixed C_3/C_4 community to a predominance of species using the C_3 photosynthetic pathway. The most straightforward interpretation of this $n\text{-C}_{31}$ $\delta^{13}\text{C}$ record is that, throughout the megadrought, the moist forest, dry forest and wooded savanna fringing Lake Chala were more established than before the drought occurred. This increase in the C_3 plant community, came at the expense of the C_4 plants occupying the understory of the dry forest and the C_4 grassland. The reconstructed 50% C_4 contribution inferred from the $\delta^{13}\text{C}$ value in surface sediments (Damsté et al., 2011) is consistent with the approximately equal abundance of C_3 and C_4 plants in the modern-day vegetation surrounding Lake Chala: broadly one quarter of the crater is occupied with moist forest dominated by C_3 plants, one third is dry C_3 forest with C_4 grasses in the understory, and roughly half is C_4 grassland with scattered C_3 trees and herbs. Henceforth amid the megadrought, the local and regional lowland vegetation was dominated by C_3 trees and shrubs, notably more so than what currently occupies the crater and surrounding landscape.

Crassulacean Acid Metabolism (CAM) plants have been found in the local dry forest and this could bias the $\delta^{13}\text{C}$ proportion of C_4 vegetation inferred in this study because, CAM plants have isotope delta values of between -10 to -20 (‰) (O'Leary, 1988), similar to that of C_4 vegetation. *Euphorbia* for example amounts to no more than 4.4% of the modern-day pollen assemblage (S. M. Rucina, National Museums of Kenya), and its pollen abundance has been relatively stable at $4.6 \pm 4\%$ throughout the Holocene (Damsté et al., 2011). Even though a species' preserved leaf-wax contribution may not match its relative pollen production, it is unlikely in this case to have affected the variations in the reconstructed $\delta^{13}\text{C}$ of $n\text{-C}_{31}$ to a large extent. In any event, CAM derived leaf waxes would have muted rather than accentuated the $\delta^{13}\text{C}$ -inferred shift to a C_3 predominated plant community.

The lack of recognisable trends in the BIT moisture balance proxy and mean insolation for 3° south (figure 4.2b and c), when compared to that of the C_3 or C_4 vegetation record is surprising (figure 4.2e and f). Noticeably though, insolation was amplified during the middle of the megadrought period (around 105 ka PB), this could mean that the increased seasonal contrast could have favoured the C_3 vegetation. Although there was reduced water levels within Lake

Chala at this time, perhaps there was sufficient moisture balance at this time to sustain significant forest cover within the region.

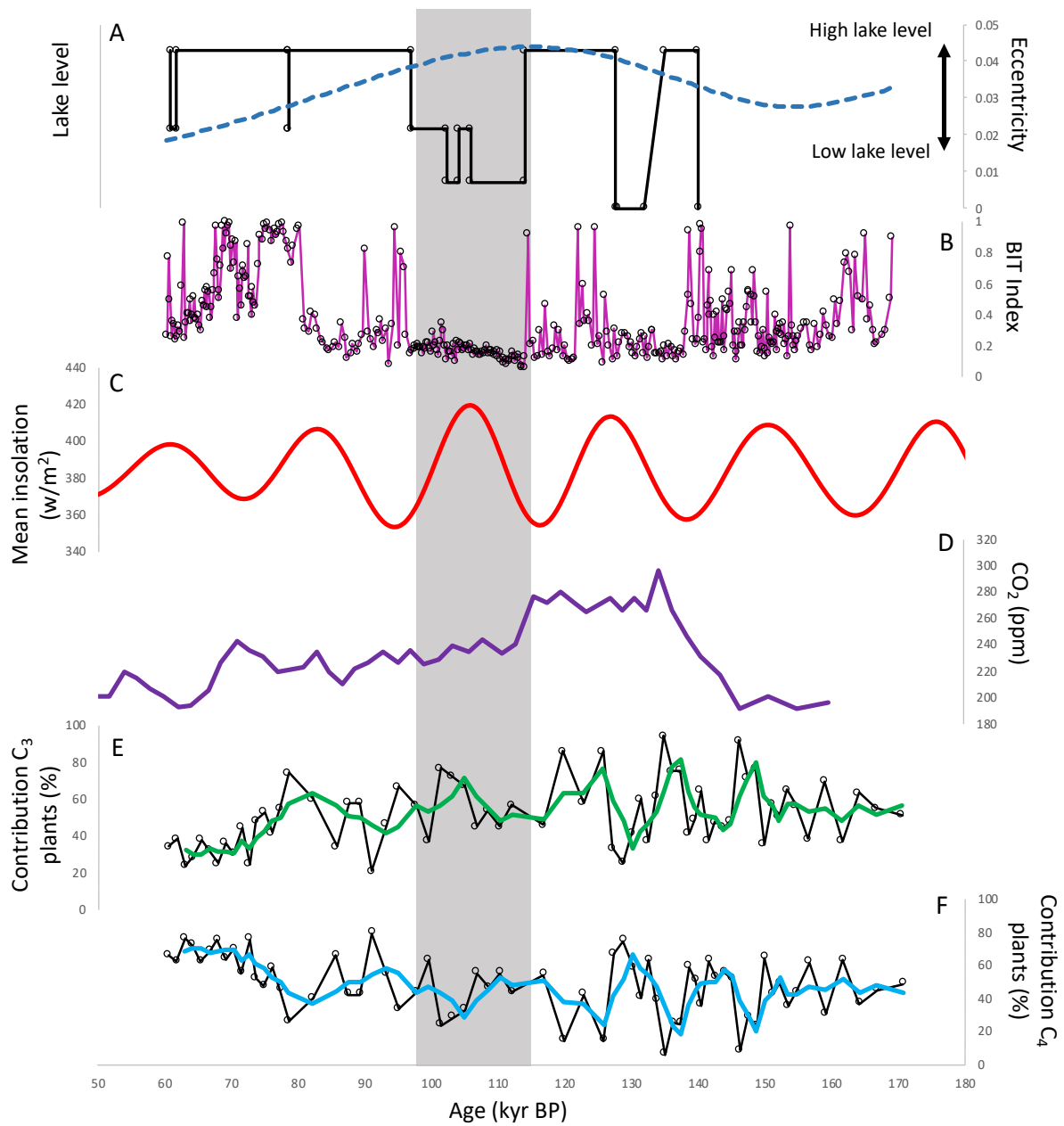


Figure 4.2 summary of lake Chala's lake level fluctuations, plotted with orbital forcing, carbon dioxide concentrations, a precipitation proxy and C_3 vs. C_4 vegetation contributions to the sediments, over the period 170.7-60.6 kyr BP. (A) The seismic-stratigraphic record of lake-level fluctuations in Lake Chala (Moernaut et al., 2010), plotted vs. Eccentricity (Berger, 1987). (B) Branched vs. isoprenoid index of tetraethers (BIT index), an indicator for monsoon rainfall intensity, (Baxter, 2018). (C) Mean insolation in (W/m^2) for 3.19° South (Berger, 1987). (D)

Global CO₂ from the Vostok ice core in (parts per million), (Barnola et al., 1987). (E) Contribution of the C₃ plants to the sedimentary n-C₃₁ alkane record (thick green line). (F) Contribution of the C₄ plants to the sedimentary n-C₃₁ alkane record (thick blue line). The thin black lines in (E-F) are the proxy records and the (thick coloured lines) represent a three-point moving average. The grey shaded area is the drought, as recognised in the seismic-stratigraphic record of lake-level fluctuations (Moernaut et al., 2010).

Curiously, vegetation records from North West Africa site GeoB9528-3 (Castaneda et al., 2009) and South East Africa sediment core MD96-2048 (Castaneda et al., 2016) during MIS 5, exhibit conflicting trends to that of this study (figure 4.3). The comparison of figures 4.3 and 4.4, reveal Northern Africa experienced dry conditions between 115 - 105 ka BP (figure 4.4), and the recorded $\delta^{13}\text{C}$ of *n*-C₃₁ from site GeoB9528-3 increased over this interval from -26.1 to -24.9‰ (figure 4.2). This shows that there was a shift to more C₄ vegetation, concurrently around the megadrought period experienced in Tropical Africa. Again, Southern Africa experienced dry conditions between 105 - 90 ka BP (Figure 4.4) and the recorded $\delta^{13}\text{C}$ of *n*-C₃₁ from sediment core MD96-2048 increased from -25.9 to -24.5‰ during this period, also suggesting an increase in the C₄ plant community. Tropical Africa experienced an extended period of aridity lasting from 115 to 90 ka BP (figure 4.4), and at Lake Chala between 115 and 101 ka BP (the most arid part indicated by the seismic-stratigraphic record of lake-level fluctuations) the $\delta^{13}\text{C}$ of *n*-C₃₁ decreased from -27.9 to -30.0‰. This implies that there was an increase in the C₃ vegetation in this region, contrary to the Northern and Southern parts of the African continent at this time.

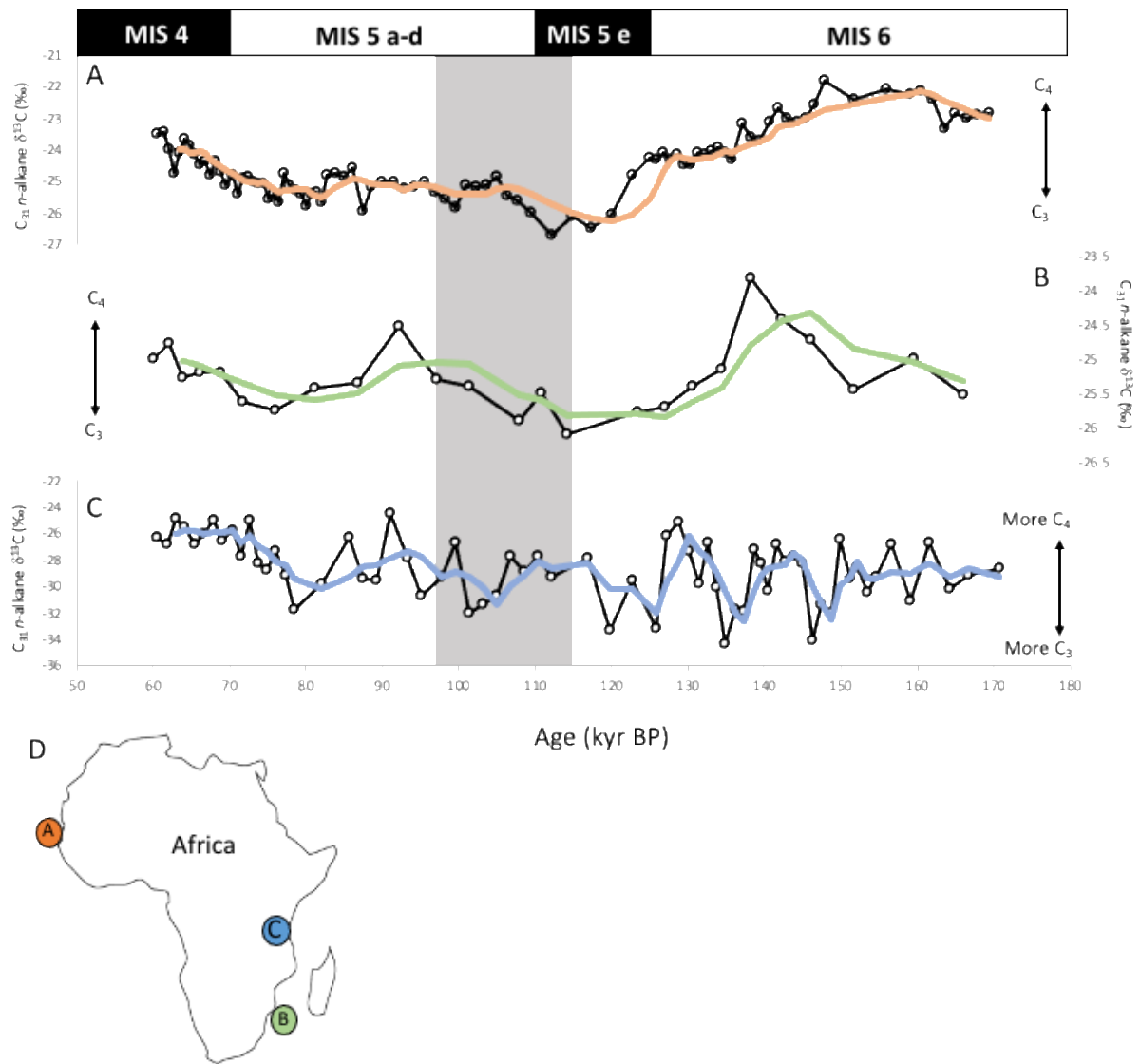


Figure 4.3 Three $\delta^{13}\text{C}_{31}$ n-alkane records from different regions of Africa over the time period 170.7-60.6 kyr BP. (A) $\delta^{13}\text{C}_{31}$ n-alkane records from North West Africa, site GeoB9528-3 (Castaneda et al., 2009). (B) $\delta^{13}\text{C}_{31}$ n-alkane records from South-East Africa, sediment core MD96-2048 (Castaneda et al., 2016). (C) $\delta^{13}\text{C}_{31}$ n-alkane records from Lake Chala (this study). The thin black lines in (A-C) are the proxy records and the (thick coloured lines) represent a three-point moving average. The grey shaded area is the drought interval, as recognised in the seismic-stratigraphic record of lake-level fluctuations (Moernaut et al., 2010). The marine isotope stages are also indicated (top). (D) Map showing the locations of the different sedimentary $\delta^{13}\text{C}_{31}$ n-alkane records.

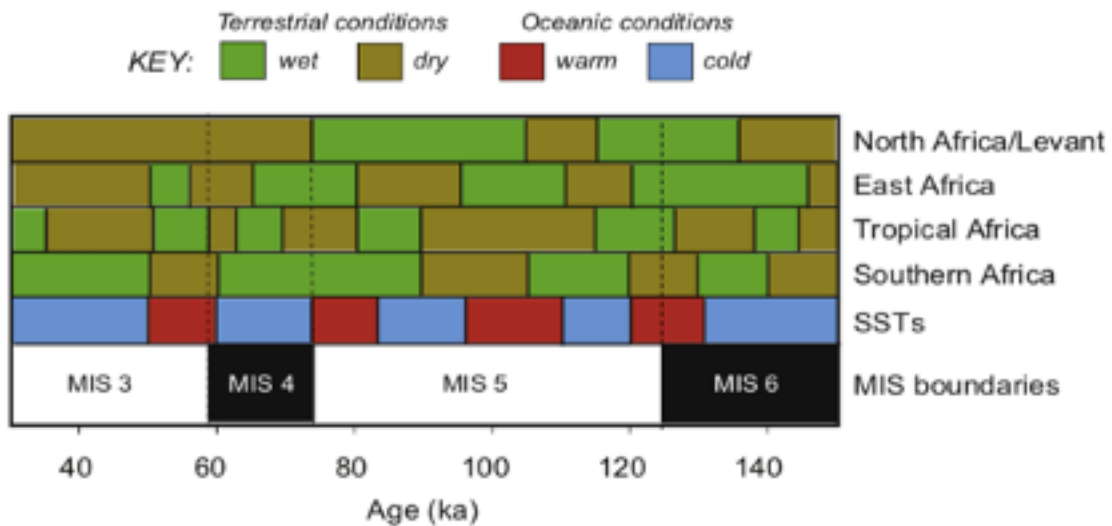


Figure 4.4 Summary of the circum-Africa climate data from 150 to 30 ka including sea surface temperatures (SSTs), compiled from 85 diverse datasets at a regional scale (Whiting Blome et al., 2012).

4.3. Climate control on temporal changes in C₃/C₄ plant contributions

Unravelling the principal climate related environmental controls on vegetation in grass-dominated biomes in tropical Africa is challenging (Wooller et al., 2003). One of the more increasingly studied time intervals used to explore this issue, is that of the Last Glacial Maximum (Wu et al., 2007; Sinninghe Damsté et al 2011; Garcin et al., 2014; Loomis et al., 2017) in part, due to the large number of available climate archives. The LGM is also a comparable time-interval for this study, because of the similar magnitude of temperature change and the associated reduction in rainfall.

Palynological studies have documented that during the LGM, moist tropical montane forest on East African mountains was replaced by cool grassland with xerophytic heather shrubs (Jolly et al., 1998) such as now occurs above the tree line. The magnitude of the reconstructed vegetation determined that the upper tree line dropped by ~1000 m on Mt. Kilimanjaro from 3200 to 2200m (Zech, 2006). Hamilton, 1972 understood this tree-line depression to have resulted entirely from lowered temperature, on the order of -6 °C. More recently pollen-based reconstructions considering the combined effect of changes in temperature and rainfall (Bonnefille et al., 1990, 1992; Vincens et al., 1993) suggested that the tree-line depression was due to glacial climate being cooler (3-4°C) and drier (30% less rainfall than average). Model simulations of the interacting effects of climate and atmospheric

CO₂ on African vegetation (Jolly and Haxeltine, 1997) showed that the mid elevation mountain site of Kashiru in Burundi (2240 m, i.e., close to the LGM treeline), the ~100 ppm reduction in glacial CO₂ alone could explain the observed replacement of moist montane forest by ericaceous shrubs. The discussion of climate versus CO₂ control on African vegetation dynamics over glacial-interglacial periods (especially during the LGM) has for the most part, focused on events in the upper tree line, this is because a large number of available continuous pollen records tend to be from mid elevation sites (~2000-3000 m, e.g., Rucina et al., 2009, Street-Perrott et al., 2007; Taylor 1990). The debate around the corresponding significance of these factors with regards to the vegetation composition in lowland African savannas, is usually framed in the modern context. This context is that the recent anthropogenic CO₂ increase, might explain the widespread encroachment of trees and shrubs into tropical savannas that has occurred in more recent times (e.g., Archer et al., 1995; Polley et al., 2002), and how future ecosystem properties and functioning could be affected by changing CO₂ (Polley et al., 1999), rainfall (Sankaran et al., 2005) and land use (Scholes and Archer, 1997). In this regard the effect of changing CO₂ concentrations, is expected to have a similar effect at all elevations on tropical African vegetation, because the partial pressures of CO₂ and O₂ both reduce with altitude (Terashima et al., 1995).

High atmospheric concentrations of CO₂ during interglacial periods as well as anthropogenically released CO₂ as stated earlier, are thought to favour C₃ trees and shrubs relatively to C₄ grasses, essentially by enabling them to limit their water loss due to transpiration under dry conditions and still absorb sufficient CO₂ to outcompete C₄ grasses (Harrison and Prentice, 2003). Although field studies by Stock et al., 2005 and Wand et al., 1999 show elevated CO₂ can also reduce transpiration by C₄ grasses. On the other hand, high levels of CO₂ may favour trees and shrubs, by increasing soil water availability (Polley et al., 1999) or by rejuvenating the regrowth of trees after fire (Bond et al., 2003). It is well understood that disturbances from fire and herbivory, strongly affect savanna vegetation dynamics (Staver et al., 2009). Fire is known to prevent large areas of savanna from reaching their maximum potential woody cover, as determined by climate (Bond et al. 2005) and shapes savanna structure and contributes to ecosystem heterogeneity (Eckhardt et al. 2000). Higgins et al., 2000, states that although fire has impacts on woody cover at landscape scales, the mechanism is demographic at the tree population level. They suggest that fires limit woody cover by preventing establishment of adult trees rather than by killing existing adult

trees. Williams et al. 1999., state this is because fire is extremely damaging too, and often kills, the shoots of tree saplings; but does far less harm to adult trees. Starver et al., 2009 state that soil resources, including nutrients and moisture, are probably instrumental in determining tree growth rates nevertheless disturbances from fire and herbivory may be instrumental in limiting tree cover and facilitating the coexistence of trees and grasses in savannas. Their model results suggest that while browsing and fire each alone impacted growth, a combination of browsing and fire had much greater effects on tree density. That being said, a recent compilation of literature by (Midgley et al., 2010) suggests that herbivory, notably by elephants and impala, can be more significant than fire alone on woody plant population size. Midgley et al., 2010, maintain the fact that the differences in strategies and responses of savanna plants to fire and herbivory are poorly explored. Indeed, the spread and decline of the tree line on Mt. Kilimanjaro since the Last Glacial oscillated depending on climate and fuel-controlled fire dynamics (Schülera et al., 2012). Whether regular fires had a stabilizing effect on lowland vegetation composition too, or whether there were sufficient water resources available to sustain large grazing herds at this time remains to be known. However, based on limited charcoal deposition in the Maundi crater sedimentological record (located at 2780 m elevation on the south-eastern slope of Mt Kilimanjaro), the cool and dry conditions of the last Glacial suggest insufficient plant fuel to maintain extensive fires (Schülera et al., 2012). The higher-plant *n*-alkane concentrations (figure 3.2) for both the C₂₉ and C₃₁ *n*-alkane were on average, significantly lower during the megadrought period 115-98 ka BP (908 µg / g and 958 µg / g *n*=11) than the succeeding time-period 98-75 ka BP (1661 µg / g and 2178 µg / g *n*=12). So, this supports the notion of insufficient plant fuel being a component during the most severe phase of aridity.

The BIOME4 coupled biogeography and biogeochemistry model (Kaplan et al., 2003) which simulates the equilibrium distribution of 28 major potential natural vegetation types from latitude, atmospheric CO₂ concentration, mean monthly climate, and soil physical properties; attributes important roles of both moisture balance and CO₂, in the expansion of drought-tolerant vegetation and the contraction of forests, across tropical Africa during the LGM (Harrison and Prentice., 2003). They came to this conclusion when simulating competition between plant functional types (PFTs) as a function of relative net primary productivity (NPP) and using an optimisation algorithm to calculate the maximum sustainable leaf area (LAI) of each PFT and its associated NPP. They then assigned biomes based on the

identity of the most successful and second-most successful PFT and their sustainable LAI. In addition, Chen et al., 2019 also found that moisture balance and CO₂ are major determinants influencing forest cover in the tropics. They showed that regional tree cover is highly regulated by mean annual precipitation (MAP), and that the threshold at which maximum tree cover is reached, is significantly reduced with elevated CO₂ for tropical and temperate trees. They also suggest that with higher CO₂, the increased tree cover leads to reduced fire ignition and burned area and provides a positive feedback to tree cover. A 25,000-year record of African lowland vegetation that covered the last glacial maximum (LGM) another similarly arid interval for tropical Africa (Sinninghe Damsté et al 2011), found that at the sub-millennial time scale, the impact of abrupt climatic moisture-balance variation on vegetation in the Lake Chala region was distinct and prominent. Intriguingly however this was not the most influential control on vegetation within the region, it instead followed the glacial/interglacial evolution of CO₂.

Sensitivity of tropical vegetation to temperature is often considered as secondary or negligible due to difficulties in reconstructing temperature in the tropics (Cohn et al., 2014). Loomis et al., 2017 found that the tropical lapse rate steepened during the Last Glacial Maximum and that cooling was amplified with elevation. This could also suggest that temperature was an important determining factor, in vegetation composition during the megadrought period because of the similar 4-6°C change in temperature (Scholz et al., 2007). Furthermore, state of the art computer models have been found to underestimate the tropical lapse-rate change (Loomis et al., 2017). Therefore, the cooler temperatures throughout the megadrought period, could have been more advantageous to the establishment of C₃ vegetation cover provided there was still sufficient moisture available for them to outcompete C₄ species.

In spite of substantial changes in moisture balance, the principal trend in C₃₁ *n*-alkane δ¹³C at Lake Chala, tracks the Pleistocene evolution in CO₂ with an inferred C₄ contribution of ~6% at 134.9 ka BP when CO₂ was at values of >290 ppm, and ~76% at 63.9 ka BP when CO₂ was at values of <200 ppm (figure 4.2d and f). The major transition from near pure C₃ vegetation cover to a more mixed C₃/C₄ vegetation started at 134.9 ka BP and moved beyond the short-term variability of δ¹³C values from 128.8 ka BP onwards, when the first prominent low stand is recorded in the seismic stratigraphic record of past lake level fluctuations (figure 4.2a). This close agreement in timing logically suggests a causal relationship and therefore

consequently a direct response of the local vegetation to carbon limitation. Straightforward comparison of the $n\text{-C}_{31}$ $\delta^{13}\text{C}$ record with the BIT rainfall record (figure 4.2b) shows little correlation on long term trends. The most severe phase of aridity at Lake Chala was between 105-115 ka as indicated by the lake-level reconstructions (Figure 4.2a) and by the BIT rainfall record (figure 4.2b). Nevertheless, C_3 contributions to the sedimentary record remain relatively stable throughout this time between 56-45%, allowing for the limited number of data points. After 105 ka lake levels began to rebound but not until 102ka did a significant increase in water volume take place, and even so the $\%C_4$ vegetation dropped even more at this time to $\sim 23\%$. This implies that moisture balance was not the primary control on the region's vegetation at this time. Secondly, there is an appreciable difference between the C_4 contribution between drier (98-115 ka; mean value 44%, $n=9$) and wetter (60-70 ka; mean value 68%, $n=9$) time intervals explored in this study. What's is more, the percentage of the C_3 contribution continues to increase throughout the megadrought time-period despite substantially reduced rainfall. This cannot be explained by unresolved issues with the BIT-inferred rainfall proxy since its temporal pattern of climatic moisture-balance change is supported by the seismic data on past lake-level fluctuations (Moernaut et al., 2010; Verschuren et al., 2009). This suggests that rainfall variation by itself is not the single most important driver of long-term vegetation change in this region of tropical Africa. In contrast the $n\text{-C}_{31}$ $\delta^{13}\text{C}$ record shows large variability between certain time intervals; 134.9 and 128.7 ka BP, and 95 and 91.1 ka BP, the measured $\delta^{13}\text{C}$ fluctuates between -36.9 and -27.7‰ and -33.3 and -26.8‰ (figure 3.4e) which correspond to $\%C_4$ changes from 6% to 75% and 33% to 79% respectively (figure 4.2f). This demonstrates that there were abrupt changes in the composition of the regions lowland vegetation and implies that moisture balance variation can have drastic effects on species composition, despite it being influenced also on longer timescales by CO_2 .

Globally, the amount and seasonality of rainfall is a primary determinant of the distribution and structure of savannas because it controls plant growth rates, productivity and fire (Archibald et al., 2013; Good and Caylor., 2011). The lack of moisture being brought from the Indian Ocean during this megadrought would have caused significant stress on the vegetation. Drought (water stress) is one of the most important environmental stresses and occurs for several reasons, including low rainfall, salinity, high and low temperatures, and high

intensity of light, among others (Salehi-Lisar and Bakhshayeshan-Agdam, 2016). Drought stress is a multidimensional stress and causes changes in the physiological, morphological, biochemical, and molecular traits in plants. It is plausible that the vegetation in this semi-arid equatorial region is less vulnerable to additional drought when CO₂ levels are relatively high. Non-CAM C₃ plants are physiologically adapted to the strongly bimodal rainfall seasonality and long dry season in this region, because of their deciduous nature and microphylls or waxy leaves (Sinninghe Damsté et al., 2011). In addition, modelling experiments have already suggested that at low CO₂ concentrations, vegetation is relatively insensitive to the exact magnitude of temperature depression (Jolly and Haxeltine, 1997) but increasingly sensitive to drought (Wu et al., 2007). It is conceivable that high CO₂ levels, could have reduced the sensitivity of C₃ vegetation to the amplified seasonal drought in this region.

In summery the extremely arid conditions in easternmost equatorial Africa during Marine Isotope Stage 5, had significant consequences for the composition of lowland vegetation. The discrete episodes of extreme drought, that were not often fully captured by the BIT rainfall proxy, created at times, a composition of vegetation that had a high proportion of C₄ species. The high atmospheric levels of CO₂ enabled C₃ trees and shrubs to be buffeted somewhat from abrupt moisture balance variations and they maintained a substantial constituent to the composition of this region's vegetation, even in the most arid phase of the megadrought period. This work demonstrates that CO₂ is just as, if not more, important than rainfall in governing vegetation patterns and contributes an important chapter in understanding vegetational influences and ecosystem thresholds, in the Pleistocene climate dynamics of tropical Africa. This study further increases our understanding of continental and equatorial climate change and sheds light on potential vegetational perturbations that could happen in the future. Albeit MIS-5 climate should not be considered as a full analogue for future climate change because of its different astronomical and greenhouse forcing's (Nikolova et al., 2013).

5. Conclusion

In conclusion, leaf-wax $\delta^{13}\text{C}$ data from lake Chala document the wide-ranging shifts in C_3/C_4 plant ratio which occurred in the savanna landscape of semi-arid easternmost equatorial Africa, within the course of the megadrought period and the transitions either side. High atmospheric CO_2 concentrations during the Late Pleistocene megadroughts, enabled C_3 trees and shrubs to outcompete C_4 grasses despite substantial moisture balance variation. The physiological adaptations of local C_3 plants to highly bimodal rainfall seasonality and an extended dry season, enabled non-CAM C_3 vegetation to become less vulnerable to additional drought stress. This study shows that tropical African vegetation is heavily influenced by climatic moisture balance change on short timescales, though on longer timescales appears to follow the main long-term trend in atmospheric CO_2 . One of the limitations of this study could be the use of the simple linear mixing model because they can fail to accurately reconstruct the relative proportions of C_3 and C_4 vegetation cover. Garcin et al., 2014, points out, that using this type of model with $\delta^{13}\text{C}$ values of sedimentary *n*-alkanes can often overestimate the proportion of C_3 vegetation, because of the differences in plant wax production, preservation, transport, and/or deposition between C_3 and C_4 plants.

References

- Albrecht, P. and Ourisson, G., (1969).** Triterpene alcohol isolation from oil shale. *Science*, **163**(3872), pp.1192-1193. DOI: 10.1126/science.163.3872.1192
- Archer, S., Schimel, D. S., & Holland, E. A. (1995).** Mechanisms of shrubland expansion: land use, climate or CO₂? *Climatic change*, **29**(1), pp.91-99. DOI: 10.1007/BF01091640
- Archibald, S., Lehmann, C.E., Gómez-Dans, J.L. and Bradstock, R.A., (2013).** Defining pyromes and global syndromes of fire regimes. *Proceedings of the National Academy of Sciences*, **110**(16), pp.6442-6447. DOI: 10.1073/pnas.1211466110
- Aucour, A.M., Hillaire-Marcel, C., and Bonnefille, R., (1994).** Late Quaternary biomass changes from 13C measurements in a highland peatbog from equatorial Africa (Burundi). *Quaternary Research*, **41**(2), pp.225-233. DOI: 10.1006/qres.1994.1024
- Barker, P.A., Hurrell, E.R., Leng, M.J., Plessen, B., Wolff, C., Conley, D.J., Keppens, E., Milne, I., Cumming, B.F., Laird, K.R., Kendrick, P., Wynn, M., and Verschuren, D., (2013).** Carbon cycling within an East African lake revealed by the carbon isotope composition of diatom silica: a 25-ka record from Lake Challa, Mt. Kilimanjaro. *Quaternary Science Reviews*, **66**, pp.55-63. DOI: 10.1016/j.quascirev.2012.07.016
- Baxter, A.J., (2018).** Investigating climate changes in East Africa during MIS5 using GDGTs from Lake Challa. Master Thesis, Utrecht University Repository.
- Baxter, A.J., (2019).** *Parallel session in paleoclimate: Lipid biomarkers in Lake Chala record African Megadroughts during MIS5.* NAC (Nederlands Aardwetenschappelijk Congres), Utrecht, delivered 15 March 2019.
- Baxter, A.J., van Bree, L.G.J., Peterse, F., Hopmans, E.C., Villanueva, L., Verschuren, D. and Damsté, J.S., (2021).** Seasonal and multi-annual variation in the abundance of isoprenoid GDGT membrane lipids and their producers in the water column of a meromictic equatorial crater lake (Lake Chala, East Africa). *Quaternary Science Reviews*, **273**, p.107263. DOI: 10.1016/j.quascirev.2021.107263
- Berger, A., (1978).** Long-term variations of daily insolation and Quaternary climatic change, *Journal of Atmospheric Science*, **35**(12), pp.2362-2367. DOI: 10.1175/1520-0469(1978)035<2362:LTVODI>2.0.CO;2
- Bianchi, T.S. and Canuel, E.A., (2011).** Chemical biomarkers in aquatic ecosystems textbook. Princeton University Press. ISBN: 9780691134147
- Blome, M.W., Cohen, A.S., Tryon, C.A., Brooks, A.S., and Russell, J., (2012).** The environmental context for the origins of modern human diversity: A synthesis of regional variability in African climate 150,000–30,000 years ago. *Journal of Human Evolution*, **62**(5), pp.563-592. DOI: 10.1016/j.jhevol.2012.01.011
- Bond, W.J., Midgley, G.F. and Woodward, F.I., (2003).** The importance of low atmospheric CO₂ and fire in promoting the spread of grasslands and savannas. *Global Change Biology*, **9**(7), pp.973-982. DOI: 10.1046/j.1365-2486.2003.00577.x
- Bond, W.J., Woodward, F.I. and Midgley, G.F., (2005).** The global distribution of ecosystems in a world without fire. *New phytologist*, **165**(2), pp.525-538. DOI: 10.1111/j.1469-8137.2004.01252.x
- Bonnefille, R., Chalié, F., Guiot, J. and Vincens, A., (1992).** Quantitative estimates of full glacial temperatures in equatorial Africa from palynological data. *Climate Dynamics*, **6**(3-4), pp.251-257. DOI: 10.1007/BF00193538
- Bonnefille, R., Roeland, J.C. and Guiot, J., (1990).** Temperature and rainfall estimates for the past 40,000 years in equatorial Africa. *Nature*, **346**(6282), pp.347-349. DOI: 10.1038/346347a0

- Bradley, R.S., Vuille, M., Diaz, H.F., and Vergara, W., (2006).** Threats to water supplies in the tropical Andes. *Science*, **312**(5781), pp.1755-1756. DOI: 10.1126/science.1128087
- Brocks, J.J., Love, G.D., Summons, R.E., Knoll, A.H., Logan, G.A., and Bowden, S.A., (2005).** Biomarker evidence for green and purple sulphur bacteria in a stratified Palaeoproterozoic sea. *Nature*, **437**(7060), p.866. DOI: 10.1038/nature04068
- Buckles, L.K., Verschuren, D., Weijers, J.W., Cocquyt, C., Blaauw, M., and Sinninghe Damsté, J.S., (2016).** Interannual and (multi-) decadal variability in the sedimentary BIT index of Lake Challa, East Africa, over the past 2200 years: assessment of the precipitation proxy. *Climate of the Past*, **12**(5), pp.1243-1262. DOI: 10.5194/cp-12-1243-2016
- Burnett, A.P., Soreghan, M.J., Scholz, C.A. and Brown, E.T., (2011).** Tropical East African climate change and its relation to global climate: a record from Lake Tanganyika, Tropical East Africa, over the past 90+ kyr. *Palaeogeography, Palaeoclimatology, Palaeoecology*, **303**(1-4), pp.155-167. DOI: 10.1016/j.palaeo.2010.02.011
- Bush, R.T. and McInerney, F.A., (2013).** Leaf wax n-alkane distributions in and across modern plants: implications for paleoecology and chemotaxonomy. *Geochimica et Cosmochimica Acta*, **117**, pp.161-179. DOI: 10.1016/j.gca.2013.04.016
- Cane, M.A., Eshel, G. and Buckland, R.W., (1994).** Forecasting Zimbabwean maize yield using eastern equatorial Pacific sea surface temperature. *Nature*, **370**(6486), pp.204-205. DOI: 10.1038/370204a0
- Carreira, R.S., Cordeiro, L.G.M.S., Bernardes, M.C., and Hatje, V., (2016).** Distribution and characterization of organic matter using lipid biomarkers: a case study in a pristine tropical bay in NE Brazil. *Estuarine, Coastal and Shelf Science*, **168**, pp.1-9. DOI: 10.1016/j.ecss.2015.11.007
- Castañeda, I.S., Mulitza, S., Schefuß, E., dos Santos, R.A.L., Damsté, J.S.S., and Schouten, S., (2009).** Wet phases in the Sahara/Sahel region and human migration patterns in North Africa. *Proceedings of the National Academy of Sciences*, **106**(48), pp. 20159-20163. DOI: 10.1073/pnas.0905771106
- Cerling, T.E., (1992).** Development of grasslands and savannas in East Africa during the Neogene. *Palaeogeography, Palaeoclimatology and Palaeoecology*, **97**(3), pp.241-247. DOI: 10.1016/0031-0182(92)90211-M
- Clayton, R.K., (1980).** *Photosynthesis: physical mechanisms and chemical patterns* (Vol. 4). Cambridge University Press. ISBN 9780521294430
- Clemens, S.C., Murray, D.W., and Prell, W.L., (1996).** Nonstationary phase of the Plio-Pleistocene Asian monsoon. *Science*, **274**(5289), pp. 943-948. DOI: 10.1126/science.274.5289.943
- Codron, J., Codron, D., Lee-Thorp, J.A., Sponheimer, M., Bond, W.J., de Ruiter, D. and Grant, R., (2005).** Taxonomic, anatomical, and spatio-temporal variations in the stable carbon and nitrogen isotopic compositions of plants from an African savanna. *Journal of Archaeological Science*, **32**(12), pp.1757-1772. DOI: 10.1016/j.jas.2005.06.006.
- Cohen, A.S., Stone, J.R., Beuning, K.R., Park, L.E., Reinthal, P.N., Dettman, D., Scholz, C.A., Johnson, T.C., King, J.W., Talbot, M.R. and Brown, E.T., (2007).** Ecological consequences of early Late Pleistocene megadroughts in tropical Africa. *Proceedings of the National Academy of Sciences*, **104**(42), pp.16422-16427. DOI: 10.1073/pnas.0703873104
- Cohen, A.S., Stone, J.R., Beuning, K.R.M., Park, L.E., Reinthal, P.N., Dettman, D., Scholz, C.A., Johnson, T.C., King, J.W., Talbot, M.R., Brown, E.T., and Ivory, S.J., (1996).** Ecological consequences of early Late Pleistocene megadroughts in tropical Africa. *Proceedings of the National Academy of Sciences*, **104**(42), pp. 16422-16427. DOI: 10.1073/pnas.0703873104

- Cohen, Y., Yalovsky, S. and Nechushtai, R., (1995).** Integration and assembly of photosynthetic protein complexes in chloroplast thylakoid membranes. *Biochimica et Biophysica Acta (BBA)-Reviews on Biomembranes*, **1241**(1), pp.1-30. DOI: 10.1016/0304-4157(94)00012-3
- Collister, J.W., Rieley, G., Stern, B., Eglinton, G., and Fry, B., (1994).** Compound-specific $\delta^{13}\text{C}$ analyses of leaf lipids from plants with differing carbon dioxide metabolisms. *Organic Geochemistry*, **21**(7), pp.619-627. DOI: 10.1016/0146-6380(94)90008-6
- Costa, K., Russell, J., Konecky, B. and Lamb, H., (2014).** Isotopic reconstruction of the African Humid Period and Congo air boundary migration at Lake Tana, Ethiopia. *Quaternary Science Reviews*, **83**, pp.58-67. DOI: 10.1016/j.quascirev.2013.10.031
- Cranwell, P.A., (1982).** Lipids of aquatic sediments and sedimenting particulates. *Progress in lipid research*, **21**(4), pp.271-308. DOI: 10.1016/0163-7827(82)90012-1
- Cranwell, P.A., (1984).** Alkyl esters, mid chain ketones and fatty acids in late glacial and postglacial lacustrine sediments. *Organic geochemistry*, **6**, pp.115-124. DOI: 10.1016/0146-6380(84)90032-9
- Damsté, J. S. S., Verschuren, D., Ossebaar, J., Blokker, J., van Houten, R., van der Meer, M. T., Plessen, B., and Schouten, S., (2011).** A 25,000-year record of climate-induced changes in lowland vegetation of eastern equatorial Africa revealed by the stable carbon-isotopic composition of fossil plant leaf waxes. *Earth and Planetary Science Letters*, **302**(1-2), pp.236-246. DOI: 10.1016/j.epsl.2010.12.025
- Damsté, J.S.S., Schouten, S., and van Duin, A.C., (2001).** Isorenieratene derivatives in sediments: possible controls on their distribution. *Geochimica et Cosmochimica Acta*, **65**(10), pp.1557-1571. DOI: 10.1016/S0016-7037(01)00549-X
- De Menocal, P.B., (1995).** Plio-pleistocene African climate. *Science*, **270**(5233), pp.53-59. DOI: 10.1126/science.270.5233.53
- Dieleman, J., Muschick, M., Nyingi, W. D., and Verschuren, D., (2019).** Species integrity and origin of *Oreochromis hunteri* (Pisces: Cichlidae), endemic to crater Lake Chala (Kenya–Tanzania). *Hydrobiologia*, **832**(1), pp.269-282. DOI: 10.1007/s10750-018-3570-7
DOI: 10.1126/science.1070057
- Duan, S. and Bianchi, T.S., (2006).** Seasonal changes in the abundance and composition of plant pigments in particulate organic carbon in the lower Mississippi and Pearl Rivers. *Estuaries and coasts*, **29**(3), pp.427-442. DOI: 10.1007/BF02784991
- Eckhardt, H.C., Van Wilgen, B.W. and Biggs, H.C., (2000).** Trends in woody vegetation cover in the Kruger National Park, South Africa, between 1940 and 1998. *African Journal of Ecology*, **38**(2), pp.108-115. DOI: 10.1046/j.1365-2028.2000.00217.x
- Eggleston, S., Schmitt, J., Bereiter, B., Schneider, R. and Fischer, H., (2016).** Evolution of the stable carbon isotope composition of atmospheric CO₂ over the last glacial cycle. *Paleoceanography*, **31**(3), pp.434-452. DOI: 10.1002/2015PA002874
- Eglinton, G. and Hamilton, R.J., (1963)** *The Distribution of Alkanes*. In Chemical plant taxonomy, Swain (Ed.) first published: 1963. pp.187-217. ISBN: 9780124143081
- Eglinton, G. and Hamilton, R.J., (1967).** Leaf epicuticular waxes. *Science*, **156**(3780), pp.1322-1335. DOI: 10.1126/science.156.3780.1322
- Eglinton, T. I. and Eglinton, G., (2008).** Molecular proxies for paleoclimatology. *Earth and Planetary Science Letters*, **275**(1-2), pp.1-16. DOI: 10.1016/j.epsl.2008.07.012

Feakins, S.J. and Eglinton, T.I., (2005). Biomarker records of late Neogene changes in northeast African vegetation. *Geology*, **33**(12), pp.977-980. DOI: 10.1130/G21814.1

Feakins, S.J., Levin, N.E., Liddy, H.M., Sieracki, A., Eglinton, T.I. and Bonnefille, R., (2013). Northeast African vegetation change over 12 million years. *Geology*, **41**(3), pp. 295-298. DOI: 10.1130/G33845.1

Felton, A.A., Russell, J.M., Cohen, A.S., Baker, M.E., Chesley, J.T., Lezzar, K.E., McGlue, M.M., Pigati, J.S., Quade, J., Stager, J.C. and Tiercelin, J.J., (2007). Paleolimnological evidence for the onset and termination of glacial aridity from Lake Tanganyika, Tropical East Africa. *Palaeogeography, Palaeoclimatology, Palaeoecology*, **252**(3-4), pp.405-423. DOI: 10.1016/j.palaeo.2007.04.003

Ficken, K.J., Li, B., Swain, D.L. and Eglinton, G., (2000). An n-alkane proxy for the sedimentary input of submerged/floating freshwater aquatic macrophytes. *Organic geochemistry*, **31**(7-8), pp.745-749. DOI: 10.1016/S0146-6380(00)00081-4

Freimuth, E.J., Diefendorf, A.F. and Lowell, T.V., (2017). Hydrogen isotopes of n-alkanes and n-alkanoic acids as tracers of precipitation in a temperate forest and implications for paleorecords. *Geochimica et Cosmochimica Acta*, **206**, pp.166-183. DOI: 10.1016/j.gca.2017.02.027Get rights and content

Garcin, Y., Schefuß, E., Schwab, V.F., Garreta, V., Gleixner, G., Vincens, A., Todou, G., Séné, O., Onana, J.M., Achoundong, G. and Sachse, D., (2014). Reconstructing C3 and C4 vegetation cover using n-alkane carbon isotope ratios in recent lake sediments from Cameroon, Western Central Africa. *Geochimica et Cosmochimica Acta*, **142**, pp.482-500. DOI: 10.1016/j.gca.2014.07.004

Gasse, F., (2000). Hydrological changes in the African tropics since the Last Glacial Maximum. *Quaternary Science Reviews*, **19**(1-5), pp.189-211. DOI: 10.1016/S0277-3791(99)00061-X

Gasse, F., Lédée, V., Massault, M. and Fontes, J.C., (1989). Water-level fluctuations of Lake Tanganyika in phase with oceanic changes during the last glaciation and deglaciation. *Nature*, **342**(6245), pp.57-59. DOI: 10.1038/342057a0
Geochemistry **15** pp.223–231. DOI: 10.1016/0146-6380(90)90001-G

Goddard, L. and Graham, N.E., (1999). Importance of the Indian Ocean for simulating rainfall anomalies over eastern and southern Africa. *Journal of Geophysical Research: Atmospheres*, **104**(D16), pp.19099-19116. DOI: 10.1029/1999JD900326

González, A.G., Barrera, J.B., Pérez, E.M.R. and Padrón, C.E.H., (1991). Chemical constituents of the lichen *Cladonia macaronesica*. *Zeitschrift für Naturforschung C*, **46**(1-2), pp.12-18. DOI: 10.1515/znc-1991-1-203

Good, S.P. and Caylor, K.K., (2011). Climatological determinants of woody cover in Africa. *Proceedings of the National Academy of Sciences*, **108**(12), pp.4902-4907. DOI: 10.1073/pnas.1013100108

Goodwin, T. W. (1980). The biochemistry of the carotenoids, 2nd ed. Chapman & Hall, London. ISBN 978-94-009-5542-4

Grimalt, J. and Albaigés, J., (1987). Sources and occurrence of C12–C22n-alkane distributions with even carbon-number preference in sedimentary environments. *Geochimica et Cosmochimica Acta*, **51**(6), pp.1379-1384. DOI: 10.1016/0016-7037(87)90322-X

Grove, M., Lamb, H., Roberts, H., Davies, S., Marshall, M., Bates, R. and Huws, D., (2015). Climatic variability, plasticity, and dispersal: A case study from Lake Tana, Ethiopia. *Journal of human evolution*, **87**, pp.32-47. DOI: 10.1016/j.jhevol.2015.07.007

Hamilton, A.C., (1972). The interpretation of pollen diagrams from highland Uganda. *Palaeoecology of Africa*, **7**(45), p.149. DOI:

- Harrison, S.P. and Prentice, C.I., (2003).** Climate and CO₂ controls on global vegetation distribution at the last glacial maximum: analysis based on palaeovegetation data, biome modelling and palaeoclimate simulations. *Global Change Biology*, **9**(7), pp.983-1004. DOI: 10.1046/j.1365-2486.2003.00640.x
- Hemp, A., (2006).** Vegetation of Kilimanjaro: hidden endemics and missing bamboo. *African Journal of Ecology*, **44**(3), pp.305-328. DOI: 10.1111/j.1365-2028.2006.00679.x
- Higgins, S. I., Bond, W. J., & Trollope, W. S. (2000).** Fire, resprouting and variability: a recipe for grass–tree coexistence in savanna. *Journal of Ecology*, **88**(2), 213-229. DOI: 10.1046/j.1365-2745.2000.00435.x
- Huang, Y., Street-Perrott, F.A., Metcalfe, S.E., Brenner, M., Moreland, M. and Freeman, K.H., (2001).** Climate change as the dominant control on glacial-interglacial variations in C₃ and C₄ plant abundance. *Science*, **293**(5535), pp.1647-1651. DOI: 10.1126/science.1060143
- Jaffé, R. and Hausmann, K.B., (1995).** Origin and early diagenesis of arborinone/isoarborinol in sediments of a highly productive freshwater lake. *Organic Geochemistry*, **22**(1), pp.231-235. DOI: 10.1016/0146-6380(95)90020-9
- Jeffrey, S.W., Mantoura, R.F.C., and Wright, S.W. (1997).** Phytoplankton pigments in oceanography: guidelines to modern methods. Monographs on Oceanographic Methodology, 10 UNESCO, Paris, France. 661 pp. ISBN 9789231032752
- Jetter, R., Kunst, L. and Samuels A.L., (2006)** *Annual Plant Reviews*, Volume **23**, Blackwell Publishing Ltd: Oxford, pp.145-181. ISBN: 978-1-405-13268-8
- Johnson T.C., Malala J.O. (2009).** Lake Turkana and Its Link to the Nile. *Monographiae Biologicae*, **89**, pp 287-304. DOI: 10.1007/978-1-4020-9726-3_15
- Johnson, T.C., Brown, E.T., McManus, J., Barry, S., Barker, P. and Gasse, F., (2002).** A high-resolution paleoclimate record spanning the past 25,000 years in southern East Africa. *Science*, **296**(5565), pp.113-132.
- Johnson, T.C., Werne, J.P., Brown, E.T., Abbott, A., Berke, M., Steinman, B.A., Halbur, J., Contreras, S., Grosshuesch, S., Deino, A. and Scholz, C.A., (2016).** A progressively wetter climate in southern East Africa over the past 1.3 million years. *Nature*, **537**(7619), p.220-224. DOI: 10.1038/nature19065
- Jolly, D. and Haxeltine, A., (1997).** Effect of low glacial atmospheric CO₂ on tropical African montane vegetation. *Science*, **276**(5313), pp.786-788. DOI: 10.1126/science.276.5313.786
- Jolly, D., Harrison, S.P., Damnati, B. and Bonnefille, R., (1998).** Simulated climate and biomes of Africa during the Late Quaternary: Comparison with pollen and lake status data. *Quaternary Science Reviews*, **17**(6-7), pp.629-657. DOI: 10.1016/S0277-3791(98)00015-8
- Kaplan, J.O., Bigelow, N.H., Prentice, I.C., Harrison, S.P., Bartlein, P.J., Christensen, T.R., Cramer, W., Matveyeva, N.V., McGuire, A.D., Murray, D.F. and Razzhivin, V.Y., (2003).** Climate change and Arctic ecosystems: 2. Modelling, paleo data-model comparisons, and future projections. *Journal of Geophysical Research: Atmospheres*, **108**(19). DOI:10.1029/2002JD002558
- Koopmans, M.P., Köster, J., Van Kaam-Peters, H.M., Kenig, F., Schouten, S., Hartgers, W.A., de Leeuw, J. and Damsté, J.S.S (1996).** Diagenetic and catagenetic products of isorenieratene: Molecular indicators for photic zone anoxia. *Geochimica et Cosmochimica Acta*, **60**(22), pp.4467-4496. DOI: 10.1016/S0016-7037(96)00238-4
- Lamb, H.F., Bates, C.R., Bryant, C.L., Davies, S.J., Huws, D.G., Marshall, M.H., Roberts, H.M. and Toland, H., (2018).** 150,000-year palaeoclimate record from northern Ethiopia supports early, multiple dispersals or modern humans from Africa. *Scientific reports*, **8**(1), 1077. DOI: 10.1038/s41598-018-19601-w

Lea, D.W., Pak, D.K., Peterson, L.C. and Hughen, K.A., (2003). Synchronicity of tropical and high-latitude Atlantic temperatures over the last glacial termination. *Science*, **301**(5638), pp.1361-1364. DOI: 10.1126/science.1088470

Leavitt, P. R., and D. A. Hodgson. (2001). Sedimentary pigments. pp. 2–21 in J. P. Smol, H.J.B. Birks and W. M. Last, eds., *Tracking environmental changes using lake sediments*. Kluwer, New York. ISBN 978-0-306-47668-6

Leng, M., Barker, P., Moorhouse, H., Lacey, J., Wolff, C., Van Daele, M., Van der Meeren, T. and Verschuren, D., (2019), DeepCHALLA—a 250,000-year record of hydroclimate from equatorial East Africa using diatom and organic isotope data. *Geophysical Research Abstracts*, **21**. DOI: 10.1016/j.quascirev.2011.01.017

Loomis, S.E., Russell, J.M., Verschuren, D., Morrill, C., De Cort, G., Damsté, J.S.S., Olago, D., Eggermont, H., Street-Perrott, F.A. and Kelly, M.A., (2017). The tropical lapse rate steepened during the Last Glacial Maximum. *Science advances*, **3**(1), p.e1600815 DOI: 10.1126/sciadv.1600815

Lyons, R.P., Scholz, C.A., Cohen, A.S., King, J.W., Brown, E.T., Ivory, S.J., Johnson, T.C., Deino, A.L., Reinthal, P.N., McGlue, M.M. and Blome, M.W., (2015). Continuous 1.3-million-year record of East African hydroclimate, and implications for patterns of evolution and biodiversity. *Proceedings of the national Academy of Sciences*, **112**(51), pp.15568-15573. DOI: 10.1073/pnas.1512864112

Mamalakis, A., Randerson, J.T., Yu, J.Y., Pritchard, M.S., Magnúsdóttir, G., Smyth, P., Levine, P.A., Yu, S. and Foufoula-Georgiou, E., (2021). Zonally contrasting shifts of the tropical rain belt in response to climate change. *Nature Climate Change*, **11**(2), pp.143-151. DOI: 10.1038/s41558-020-00963-x

Martin-Jones, C., Lane, C., Van Daele, M., Meeren, T.V.D., Wolff, C., Moorhouse, H., Tomlinson, E. and Verschuren, D., (2019). History of scoria-cone eruptions on the eastern shoulder of the Kenya–Tanzania Rift revealed in the 250-ka sediment record of Lake Chala near Mount Kilimanjaro. *Journal of Quaternary Science*. **35**(1-2), pp.245-255. DOI: 10.1002/jqs.3140

Marzi, R., Torkelson, B.E. and Olson, R.K., (1993). A revised carbon preference index. *Organic Geochemistry*, **20**(8), pp.1303-1306. DOI: 10.1016/0146-6380(93)90016-5

Maslin, M.A. and Trauth, M.H., (2009). Plio-Pleistocene East African pulsed climate variability and its influence on early human evolution. In *The First Humans—Origin and Early Evolution of the Genus Homo* (pp. 151-158). DOI: 10.1007/978-1-4020-9980-9_13

McDonough, M.M., Šumbera, R., Mazoch, V., Ferguson, A.W., Phillips, C.D. and Bryja, J., (2015). Multilocus phylogeography of a widespread savanna–woodland-adapted rodent reveals the influence of Pleistocene geomorphology and climate change in Africa's Zambezi region. *Molecular ecology*, **24**(20), pp.5248-5266. DOI: 10.1111/mec.13374

McDougall, I., Brown, F.H. and Fleagle, J.G., (2005). Stratigraphic placement and age of modern humans from Kibish, Ethiopia. *Nature*, **433**(7027), pp.733-736. DOI: 10.1038/nature03258

Meyer, I., Van Daele, M., Tanghe, N., De Batist, M. and Verschuren, D., (2020). Reconstructing East African monsoon variability from grain-size distributions: Endmember modelling and source attribution of diatom-rich sediments from Lake Chala. *Quaternary Science Reviews*, **247**, p.106574. DOI: 10.1016/j.quascirev.2020.106574

Meyers P.A., Teranes J.L. (2002) Sediment Organic Matter. In: Last W.M., Smol J.P. (eds) *Tracking Environmental Change Using Lake Sediments. Developments in Paleoenvironmental Research*, vol **2**. Springer, Dordrecht. DOI: 10.1007/0-306-47670-3_9

Meyers, P.A. and Ishiwatari, R., (1993). Lacustrine organic geochemistry—an overview of indicators of organic matter sources and diagenesis in lake sediments. *Organic geochemistry*, **20**(7), pp.867-900. DOI: 10.1016/0146-6380(93)90100-P

- Meyers, P.A., (1997).** Organic geochemical proxies of paleoceanographic, paleolimnologic, and paleoclimatic processes. *Organic geochemistry*, **27**(5-6), pp.213-250. DOI: 10.1016/S0146-6380(97)00049-1
- Midgley, J., Lawes, M.J., and Chamaillé-Jammes, S., (2010).** Savanna woody plant dynamics: the role of fire and herbivory, separately and synergistically. *Australian Journal of Botany* **58**(1), pp.1-11. DOI: 10.1071/BT09034
- Moernaut, J., Verschuren, D., Charlet, F., Kristen, I., Fagot, M. and De Batist, M., (2010).** The seismic-stratigraphic record of lake-level fluctuations in Lake Challa: Hydrological stability and change in equatorial East Africa over the last 140 kyr. *Earth and Planetary Science Letters*, **290**(1-2), pp.214-223. DOI: 10.1016/j.epsl.2009.12.023
- Morrissey, A. and Scholz, C.A., (2014).** Paleohydrology of Lake Turkana and its influence on the Nile River system. *Palaeogeography, Palaeoclimatology, Palaeoecology*, **403**, pp.88-100. DOI: 10.1016/j.palaeo.2014.03.029
- Nikolova, I., Yin, Q., Berger, A., Singh, U.K. and Karami, M.P., (2013).** The last interglacial (Eemian) climate simulated by LOVECLIM and CCSM3. *Climate of the Past*, **9**(4), pp.1789-1806. DOI: 10.5194/cp-9-1789-2013
- Nishimura, M. and Baker, E.W., (1986).** Possible origin of n-alkanes with a remarkable even-to-odd predominance in recent marine sediments. *Geochimica et Cosmochimica Acta*, **50**(2), pp.299-305. DOI: 10.1016/0016-7037(86)90178-X
- O'Leary, M.H., (1988).** Carbon isotopes in photosynthesis. *Bioscience*, **38**(5), pp.328-336. DOI: 10.2307/1310735
- O'leary, M.H., Madhavan, S. and Paneth, P., (1992).** Physical and chemical basis of carbon isotope fractionation in plants. *Plant, Cell & Environment*, **15**(9), pp.1099-1104. DOI: 10.1111/j.1365-3040.1992.tb01660.x
- Ohmoto, T., Ikuse, M. and Natori, S., (1970).** Triterpenoids of the Gramineae. *Phytochemistry*, **9**(10), pp.2137-2148. DOI: 10.1016/S0031-9422(00)85379-0
- Olago, D.O., Street-Perrott, F.A., Perrott, R.A., Ivanovich, M., Harkness, D.D., (1999).** Late Quaternary glacial-interglacial cycle of climatic and environmental change on Mount Kenya, Kenya. *Journal of African Earth Sciences*, **29**(3), pp.593-618. DOI: 10.1016/S0899-5362(99)00117-7
- Otto-Bliesner, B.L., Russell, J.M., Clark, P.U., Li, Z., Overpeck, J.T., Konecky, B., Demenocal, P., Nicholson, S.E., He, F. and Lu, Z., (2014).** Coherent changes of southeastern equatorial and northern African rainfall during the last deglaciation. *Science*, **346**(6214), pp.1223-1227. DOI: 10.1126/science.1259531
- Ourisson, G., Albrecht, P. and Rohmer, M., (1982).** Predictive microbial biochemistry—from molecular fossils to prokaryotic membranes. *Trends in Biochemical Sciences*, **7**(7), pp.236-239. DOI: 10.1016/0968-0004(82)90028-7
- Payne, B. R., (1970).** Water balance of Lake Chala and its relation to groundwater from tritium and stable isotope data. *Journal of Hydrology*, **11**(1), pp.47-58. DOI: 10.1016/0022-1694(70)90114-9
- Peter, B.D., (2004).** African climate change and faunal evolution during the Pliocene–Pleistocene. *Earth and Planetary Science Letters*, **220**(1-2), pp.3-24. DOI: 10.1016/S0012-821X(04)00003-2
- Peterson, L.C., Haug, G.H., Hughen, K.A. and Röhl, U., (2000).** Rapid changes in the hydrologic cycle of the tropical Atlantic during the last glacial. *Science*, **290**(5498), pp.1947-1951. DOI: 10.1126/science.290.5498.1947
- Petit, J. R., Jouzel, J., Raynaud, D., Barkov, N. I., Barnola, J. M., Basile, I., Bender, M., Chappellaz, J., Davis, M., Delaygue, G., Delmotte, M., Kotlyakov, V. M., Legrand, M., Lipenkov, V. Y., Lorius, C., Pepin, L., Ritz, C., Saltzman, E., and Stevenard, M., (1999).** Climate and atmospheric history of the past 420,000 years from the Vostok ice core, Antarctica. *Nature*, **399**, pp.429–436. DOI: 10.1038/20859

Polley, H. W., Tischler, C. R., Johnson, H. B., & Derner, J. D. (2002). Growth rate and survivorship of drought: CO₂ effects on the presumed trade-off in seedlings of five woody legumes. *Tree Physiology*, **22**(6), pp.383-391. DOI: 10.1093/treephys/22.6.383

Polley, H. W., Tischler, C. R., Johnson, H. B., & Pennington, R. E. (1999). Growth, water relations, and survival of drought-exposed seedlings from six maternal families of honey mesquite (*Prosopis glandulosa*): responses to CO₂ enrichment. *Tree Physiology*, **19**(6), pp. 359-366. DOI: 10.1093/treephys/19.6.359

Potts, R., (1998). Variability selection in hominid evolution. *Evolutionary Anthropology: Issues, News, and Reviews*, **7**(3), pp.81-96. DOI: 10.1002/(SICI)1520-6505(1998)7:3<81::AID-EVAN3>3.0.CO;2-A pp.271–308. DOI: 10.1016/0163-7827(82)90012-1.

Rogge, W.F., Medeiros, P.M. and Simoneit, B.R., (2007). Organic marker compounds in surface soils of crop fields from the San Joaquin Valley fugitive dust characterization study. *Atmospheric Environment*, **41**(37), pp.8183-8204. DOI: 10.1016/j.atmosenv.2007.06.030

Rommerskirchen, F., Eglinton, G., Dupont, L. and Rullkötter, J., (2006). Glacial/interglacial changes in southern Africa: Compound-specific $\delta^{13}C$ land plant biomarker and pollen records from southeast Atlantic continental margin sediments. *Geochemistry, Geophysics, Geosystems*, **7**(8). DOI: 10.1029/2005GC001223

Rosignol-Strick, M., (1985). Mediterranean Quaternary sapropels, an immediate response of the African monsoon to variation of insolation. *Palaeogeography, palaeoclimatology, palaeoecology*, **49**(3-4), pp.237-263. DOI: 10.1016/0031-0182(85)90056-2

Rucina, S.M., Muiruri, V.M., Kinyanjui, R.N., McGuinness, K. and Marchant, R., (2009). Late Quaternary vegetation and fire dynamics on Mount Kenya. *Palaeogeography, Palaeoclimatology, Palaeoecology*, **283**(1-2), pp.1-14. DOI: 10.1016/j.palaeo.2009.08.008

Sage, R.F., Wedin, D.A. and Li, M., (1999). The biogeography of C₄ photosynthesis: patterns and controlling factors. *C₄ plant biology*, **10**, pp.313-376. DOI: 10.1016/B978-012614440-6/50011-2

Salehi-Lisar, S.Y. and Bakhshayeshan-Agdam, H., (2016). Drought stress in plants: causes, consequences, and tolerance. In *Drought Stress Tolerance in Plants*, **1** pp. 1-16. DOI: 10.1007/978-3-319-28899-4_1

Sankaran, M., Hanan, N.P., Scholes, R.J., Ratnam, J., Augustine, D.J., Cade, B.S., Gignoux, J., Higgins, S.I., Le Roux, X., Ludwig, F., Ardo, J., Banyikwa, F., Bronn, A., Bucini, G., Caylor, K.K., Coughenour, M.B., Diouf, A., Ekaya, W., Feral, C.J., February, E.C., Frost, P.G.H., Hiernaux, P., Hrabar, H., Metzger, K.L., Prins, H.H.T., Ringrose, S., Sea, W., Tews, J., Worden, J., Zambatis, N., (2005). Determinants of woody cover in African savannas. *Nature* **438**, pp. 846–849. DOI: 10.1038/nature04070

Schefuß, E., Schouten, S., Jansen, J.F. and Damsté, J.S.S., (2003). African vegetation controlled by tropical sea surface temperatures in the mid-Pleistocene period. *Nature*, **422**(6930), pp.418-421. DOI: 10.1038/nature01500

Scholes, R. J., & Archer, S. R. (1997). Tree-grass interactions in savannas. *Annual review of Ecology and Systematics*, **28**(1), pp.517-544. DOI: 10.1146/annurev.ecolsys.28.1.517

Scholz, C.A., Johnson, T.C., Cohen, A.S., King, J.W., Peck, J.A., Overpeck, J.t., Talbot, M.R., Brown, E.T., Kalindekaffe, L., Amoako, P.Y.O., Lyons, R.P., Shanahan, M.t., Castañeda, I.S., Heil, C.W., Forman, S.I., McHargue, L.R., Beuning, K.R., Gomez, J. and Pierson, J., (2007). East African megadroughts between 135 and 75 thousand years ago and bearing on early-modern human origins. *Proceedings of the National Academy of Sciences*, **104**(42), pp.16416-16421. DOI: 10.1073/pnas.0703874104

Scholz, C.A., Johnson, T.C., King, J., Cohen, A.S., Lyons, R.P., Kalindekaffe, L., Forman, S.L., McHargue, L.R. and Singer, B.S., (2005). Initial results of scientific drilling on Lake Malawi, East African rift. *American Geophysical Union, Fall Meeting 2005*, abstract id. PP13C-03, Bibcode: 2005AGUFMPP13C..03S.

- Schüler, L., Hemp, A., Zech, W., & Behling, H. (2012).** Vegetation, climate and fire-dynamics in East Africa inferred from the Maundi crater pollen record from Mt Kilimanjaro during the last glacial–interglacial cycle. *Quaternary Science Reviews*, **39**, pp.1-13. DOI: 10.1016/j.quascirev.2012.02.003
- Shaw, P.M. and Johns, R.B., (1985).** Organic geochemical studies of a recent Inner Great Barrier Reef sediment—I. Assessment of input sources. *Organic geochemistry*, **8**(2), pp.147-156. DOI: 10.1016/0146-6380(85)90032-4
- Shiea, J., Brassell, S.C. and Ward, D.M., (1990).** Mid-chain branched mono- and dimethyl alkanes in hot spring cyanobacterial mats: a direct biogenic source for branched alkanes in ancient sediments? *Organic Geochemistry*, **15**(3), pp.223-231. DOI: 10.1016/0146-6380(90)90001-G
- Smith, F. and Freeman. K., (2006).** Influence of physiology and climate on δD of leaf wax *n*-alkanes from C3 and C4 grasses. *Geochimica et tamochimca Acta*, **70**, pp.1172-1187. DOI: 10.1016/j.gca.2005.11.006
- Soden, B.J. and Held, I.M., (2006).** An assessment of climate feedbacks in coupled ocean–atmosphere models. *Journal of Climate*, **19**(14), pp.3354-3360. DOI: 10.1175/JCLI3799.1
- spring cyanobacterial mats: A direct biogenic source for branched alkanes in ancient sediments? *Organic*
- Stager, J.C., Cumming, B. and Meeker, L., (1997).** A high-resolution 11,400-yr diatom record from Lake Victoria, East Africa. *Quaternary research*, **47**(1), pp.81-89. DOI: 10.1006/qres.1996.1863
- Staver, A.C., Bond, W.J., Stock, W.D., Van Rensburg, S.J., Waldram, M.S., (2009).** Browsing and fire interact to suppress tree density in an African savanna. *Ecological Applications*, **19**(7), pp.1909-1919. DOI: 10.1890/08-1907.1
- Stock, W.D., Ludwig, F., Morrow, C., Midgley, G.F., Wand, S.J., Allsopp, N. and Bell, T.L., (2005).** Long-term effects of elevated atmospheric CO₂ on species composition and productivity of a southern African C4 dominated grassland in the vicinity of a CO₂ exhalation. *Plant Ecology*, **178**(2), pp.211-224. DOI: 10.1007/s11258-004-3654-5
- Street-Perrott, F.A. and Perrott, R.A., (1990).** Abrupt climate fluctuations in the tropics: the influence of Atlantic Ocean circulation. *Nature*, **343**(6259), pp.607-612. DOI: 10.1038/343607a0
- Street-Perrott, F.A., Barker, P.A., Swain, D.L., Ficken, K.J., Wooller, M.J., Olago, D.O. and Huang, Y., (2007).** Late Quaternary changes in ecosystems and carbon cycling on Mt. Kenya, East Africa: a landscape-ecological perspective based on multi-proxy lake-sediment influxes. *Quaternary Science Reviews*, **26**(13-14), pp.1838-1860. DOI: 10.1016/j.quascirev.2007.02.014
- Street-Perrott, F.A., Huang, Y., Perrott, R.A., Eglinton, G., Barker, P., Khelifa, L.B., Harkness, D.D. and Olago, D.O., (1997).** Impact of lower atmospheric carbon dioxide on tropical mountain ecosystems. *Science*, **278**(5342), pp.1422-1426. DOI: 10.1126/science.278.5342.1422
- Talbot, M.R. and Brendeland, K.I., (2001).** Strontium isotopes as palaeohydrological tracers in the White Nile headwater lakes, East Africa. *American Geophysical Union, Fall Meeting 2001*, abstract id. PP21C-05, Bibcode: 2001AGUFMPP21C..05T.
- Talbot, M.R. and Johannessen, T., (1992).** A high resolution palaeoclimatic record for the last 27,500 years in tropical West Africa from the carbon and nitrogen isotopic composition of lacustrine organic matter. *Earth and Planetary Science Letters*, **110**(1-4), pp.23-37. DOI: 10.1016/0012-821X(92)90036-U
- Taylor, D.M., (1990).** Late quaternary pollen records from two Ugandan mires: evidence for environmental changes in the Rukiga highlands of southwest Uganda. *Palaeogeography, Palaeoclimatology, Palaeoecology*, **80**(3-4), pp.283-300. DOI: 10.1016/0031-0182(90)90138-W
- Terashima, I., Masuzawa, T., Ohba, H., & Yokoi, Y. (1995).** Is photosynthesis suppressed at higher elevations due to low CO₂ pressure? *Ecology*, **76**(8), pp.2663-2668. DOI: 10.2307/2265838

- Thompson, L.G., Mosley-Thompson, E., Davis, M.E. and Brecher, H.H., (2011).** Tropical glaciers, recorders and indicators of climate change, are disappearing globally. *Annals of Glaciology*, **52**(59), pp.23-34. DOI: 10.3189/172756411799096231
- Tierney, J. E. and Zander, P. D., (2017).** A climatic context for the out-of-Africa migration. *Geology*, **45**(11), pp.1023-1026. DOI: 10.1130/G39457.1
- Tierney, J.E., Russell, J.M. and Huang, Y., (2010).** A molecular perspective on Late Quaternary climate and vegetation change in the Lake Tanganyika basin, East Africa. *Quaternary Science Reviews*, **29**(5-6), pp.787-800. DOI: 10.1016/j.quascirev.2009.11.030
- Tierney, J.E., Russell, J.M., Damsté, J.S.S., Huang, Y. and Verschuren, D., (2011).** Late Quaternary behaviour of the East African monsoon and the importance of the Congo Air Boundary. *Quaternary Science Reviews*, **30**(7-8), pp.798-807. DOI: 10.1016/j.quascirev.2011.01.017
- Trauth, M.H., Deino, A.L., Bergner, A.G. and Strecker, M.R., (2003).** East African climate change and orbital forcing during the last 175 kyr BP. *Earth and Planetary Science Letters*, **206**(3-4), pp.297-313. DOI: 10.1016/S0012-821X(02)01105-6
- Trauth, M.H., Maslin, M.A., Deino, A. and Strecker, M.R., (2005).** Late cenozoic moisture history of East Africa. *Science*, **309**(5743), pp.2051-2053. DOI: 10.1126/science.1112964
- Uno, K.T., Polissar, P.J. and Jackson, K.E., (2016).** Neogenic biomarker record of vegetation change in eastern Africa. *Proceedings of the National Academy of Sciences*, **113**(23), pp. 6355-6363. DOI: 10.1073/pnas.1521267113
- Van Bree, L.G.J., Islam, M.M., Rijpstra, W.I.C., Verschuren, D., van Duin, A.C.T., Damsté, J.S. and de Leeuw, J.W., (2018).** Origin, formation and environmental significance of des-A-arborenes in the sediments of an East African crater lake. *Organic Geochemistry*, **125**, pp.95-108. DOI: 10.1016/j.orggeochem.2018.09.001
- Verschuren, D., Damsté, J.S.S., Moernaut, J., Kristen, I., Blaauw, M., Fagot, M., Haug, G.H., van Geel, B., De Batist, M., Barker, P. and Vuille, M., (2009).** Half-precessional dynamics of monsoon rainfall near the East African Equator. *Nature*, **462**(7273), pp.637-641. DOI: 10.1038/nature08520
- Vincens, A., Chalié, F., Bonnefille, R., Guiot, J. and Tiercelin, J.J., (1993).** Pollen-derived rainfall and temperature estimates from Lake Tanganyika and their implication for Late Pleistocene water levels. *Quaternary Research*, **40**(3), pp.343-350. DOI: 10.1006/qres.1993.1087
- Viso, A.-C., D. Pesando, P. Bernard, and J.-C. Marty., (1993).** Lipid components of the Mediterranean seagrass
- Vogts, A., Schefuß, E., Badewien, T., Rullkötter, J. (2012).** n-Alkane parameters from a deep-sea sediment transect off southwest Africa reflect continental vegetation and climate conditions. *Organic Geochemistry*, **47**, pp.109-119. DOI: 10.1016/j.orggeochem.2012.03.011
- Volkman, J.K., (2005).** Sterols and other triterpenoids: source specificity and evolution of biosynthetic pathways. *Organic geochemistry*, **36**(2), pp.139-159. DOI: 10.1016/j.orggeochem.2004.06.013
- Wakeham, S.G. and Carpenter, R., (1976).** Aliphatic hydrocarbons in sediments of Lake Washington 1. *Limnology and oceanography*, **21**(5), pp.711-723. DOI: 10.4319/lo.1976.21.5.0711
- Wand, S.J., Midgley, G.F., Jones, M.H. and Curtis, P.S., (1999).** Responses of wild C4 and C3 grass (Poaceae) species to elevated atmospheric CO2 concentration: a meta-analytic test of current theories and perceptions. *Global Change Biology*, **5**(6), pp.723-741. DOI: 10.1046/j.1365-2486.1999.00265.x
- Weijers, J.W., Schefuß, E., Schouten, S. and Damsté, J.S.S., (2007).** Coupled thermal and hydrological evolution of tropical Africa over the last deglaciation. *Science*, **315**(5819), pp.1701-1704. DOI: 10.1126/science.1138131

White, F., (1983). *The vegetation of Africa: A Descriptive Memoir to Accompany the Unesco/AETFAT/UNSO Vegetation Map of Africa.* (Vol. 20) UNESCO, 7 Place de Fontenoy, 75700 Paris. ISBN: 9231019554

Williams, R.J., Cook, G.D., Gill, A.M. and Moore, P.H.R., (1999). Fire regime, fire intensity and tree survival in a tropical savanna in northern Australia. *Australian Journal of Ecology*, **24**(1), pp.50-59. DOI: 10.1046/j.1442-9993.1999.00946.x

Wolff, C., Kristen-Jenny, I., Schettler, G., Plessen, B., Meyer, H., Dulski, P., Naumann, R., Brauer, A., Verschuren, D. and Haug, G.H., (2014). Modern seasonality in Lake Challa (Kenya/Tanzania) and its sedimentary documentation in recent lake sediments. *Limnology and Oceanography*, **59**(5), pp.1621-1636. DOI: 10.4319/lo.2014.59.5.1621

Wooller, M.J., Swain, D.L., Ficken, K.J., Agnew, A.D.Q., Street-Perrott, F.A. and Eglinton, G., (2003). Late Quaternary vegetation changes around Lake Rutundu, Mount Kenya, East Africa: evidence from grass cuticles, pollen and stable carbon isotopes. *Journal of Quaternary Science: Published for the Quaternary Research Association*, **18**(1), pp.3-15. DOI: 10.1002/jqs.725

Wu, H., Guiot, J., Brewer, S. and Guo, Z., (2007). Climatic changes in Eurasia and Africa at the last glacial maximum and mid-Holocene: reconstruction from pollen data using inverse vegetation modelling. *Climate Dynamics*, **29**(2), pp.211-229. DOI: 10.1007/s00382-007-0231-3

Zech, M., (2006). Evidence for Late Pleistocene climate changes from buried soils on the southern slopes of Mt. Kilimanjaro, Tanzania. *Palaeogeography, Palaeoclimatology, Palaeoecology*, **242**(3-4), pp.303-312. DOI: 10.1016/j.palaeo.2006.06.008

Zheng, Y., Zhou, W., Xie, S. and Yu, X., (2009). A comparative study of n-alkane biomarker and pollen records: an example from southern China. *Chinese Science Bulletin*, **54**(6), pp.1065-1072. DOI: 10.1007/s11434-008-0563-3